Theory of Gamma Ray Bursts

Theory of Gamma Ray Bursts

Chuck Dermer **(Naval Research Laboratory, Washington DC)**

thanks to Reinhard Schlickeiser

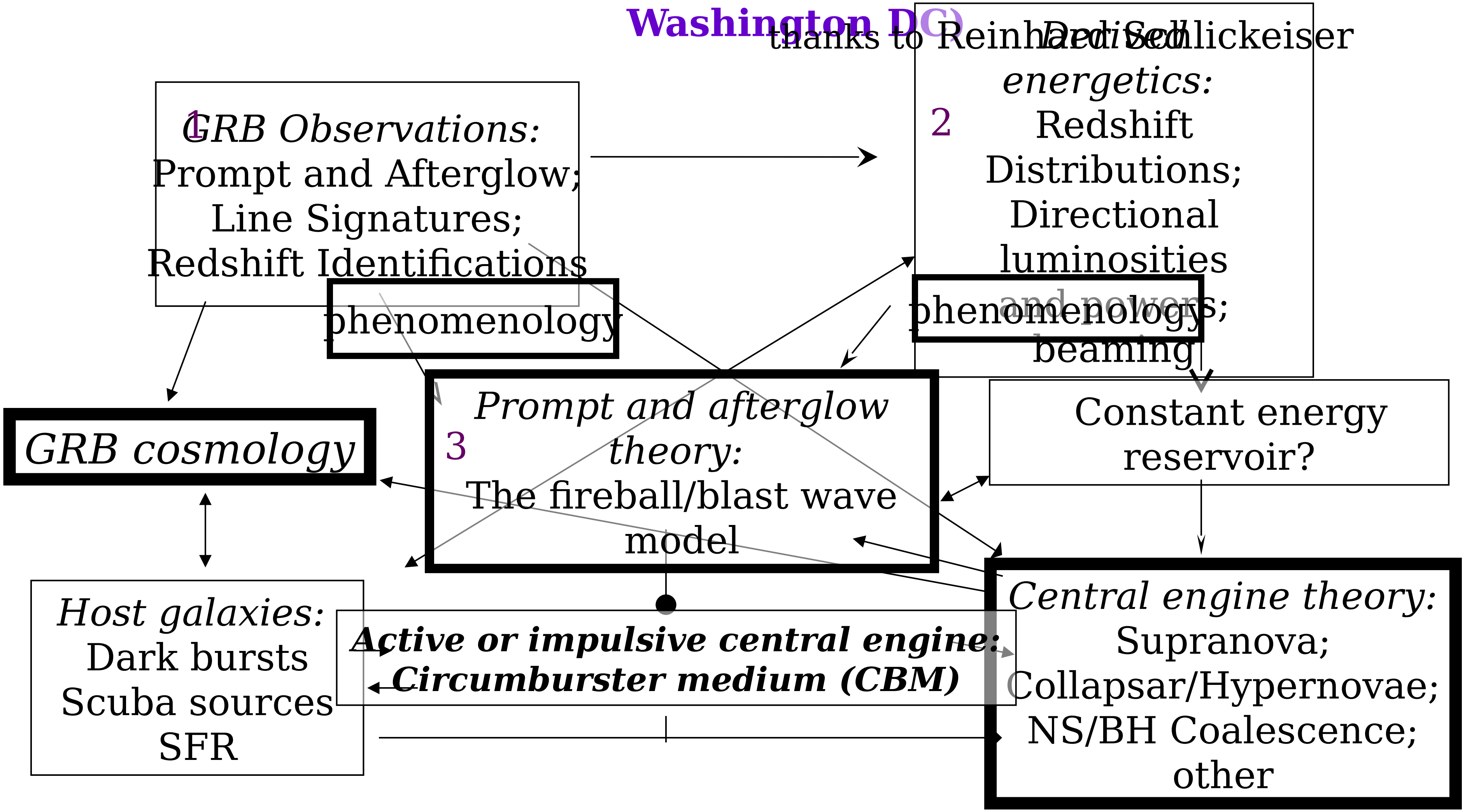

Theory of Gamma Ray Bursts

Chuck Dermer **(Naval Research Laboratory, Washington DC)**

thanks to Reinhard Schlickeiser

Cosmic Rays and High-Energy Neutrinos

Galaxy Studies;
Star formation;
Biological effects

Observations:
Prompt and Afterglow;
Line Signatures;
Redshift Identifications

phenomenology

Derived energetics:
Redshift Distributions;
Directional luminosities and powers; beaming

phenom.

GRB cosmology

Prompt and afterglow theory:
The fireball/blast wave model

Constant energy reservoir?

Host galaxies:
Dark bursts
Scuba sources
SFR

Active or impulsive central engine; Circumburster medium (CBM)

Central engine theory:
Supranova;
Collapsar/Hypernovae;
NS/BH Coalescense;
other

GRB 990123

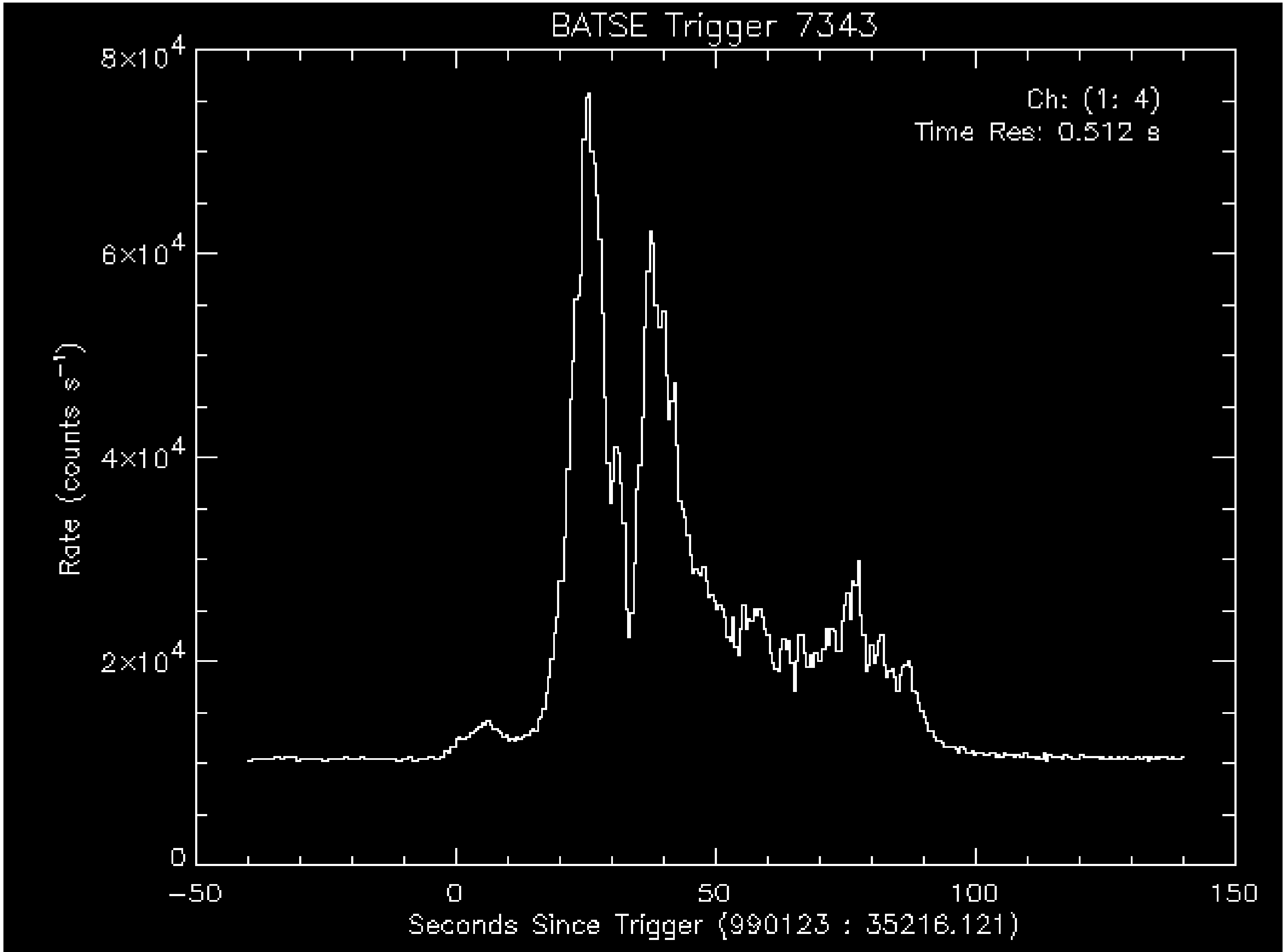

BATSE Trigger 7343
Ch: (1: 4)
Time Res: 0.512 s
Rate (counts s^{-1})
8×10^4
6×10^4
4×10^4
2×10^4
0
−50
0
50
100
150
Seconds Since Trigger (990123 : 35216.121)

GRBs: Light Curves, Durations and Peak Energy Distributions

Sample of Different GRB Light Curves

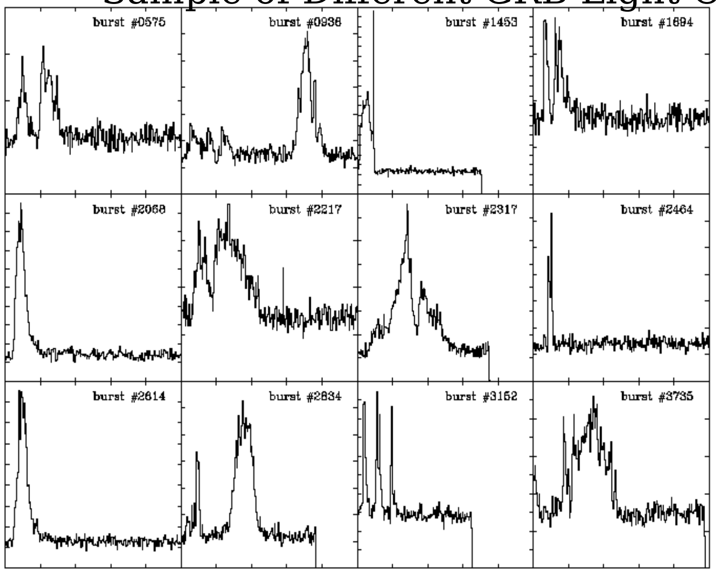

0 2 4 6
8
t (s)

BATSE triggering: 64, 256, 1024 ms

> 0.5 ph cm^{-2} s^{-1} in 50-300 keV band

$\Rightarrow$ 10 sec sensitivity $\approx 10^{7}$ ergs cm^{-2} s^{-1}

$n\sigma = S/\sqrt{B}$

GRB Duration Distribution

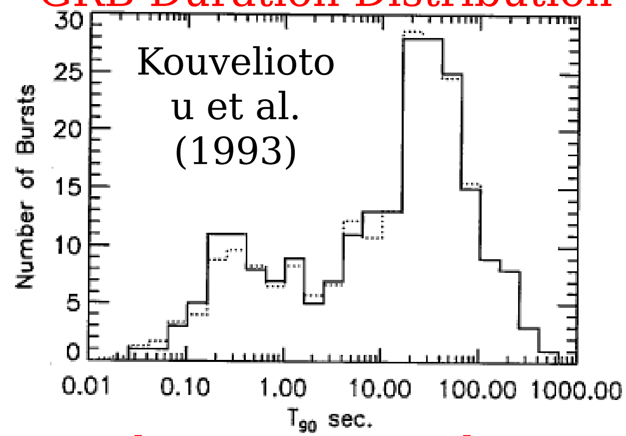

Kouveliotou et al. (1993)

Spectra E_{pk} = Peak energy of νF_ν Distribution

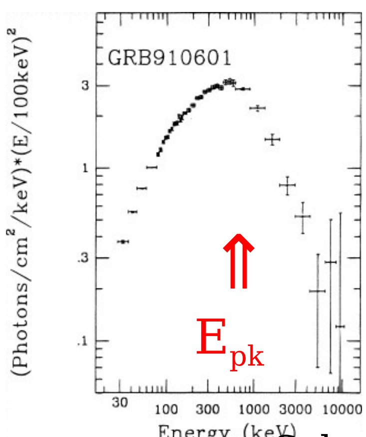

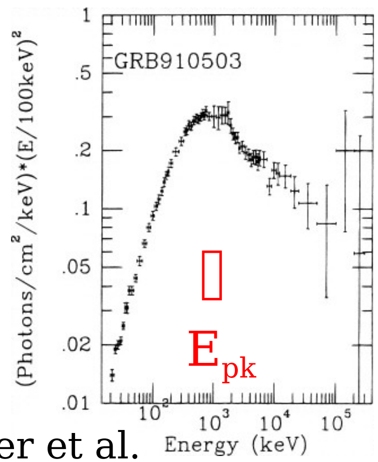

Schaefer et al. (1998)

Peak Energy Distribution

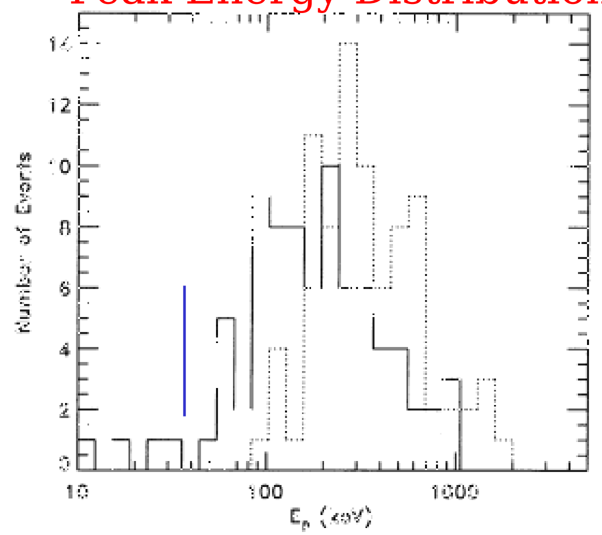

Mallozzi et al. (1997)

Size Distribution

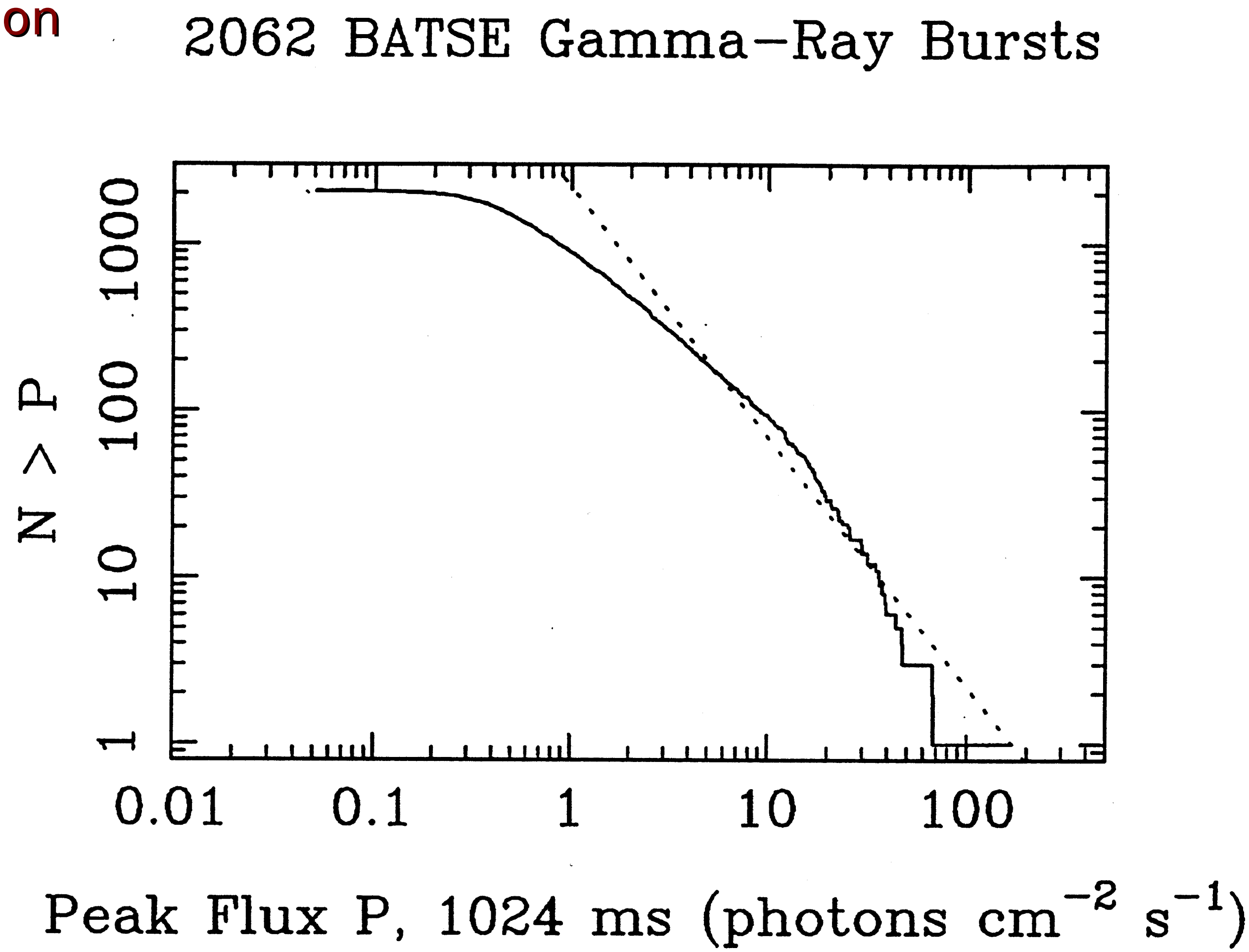

No evidence of –3/2 Euclidean slope at bright end of BATSE peak flux distribution

Afterglow observations

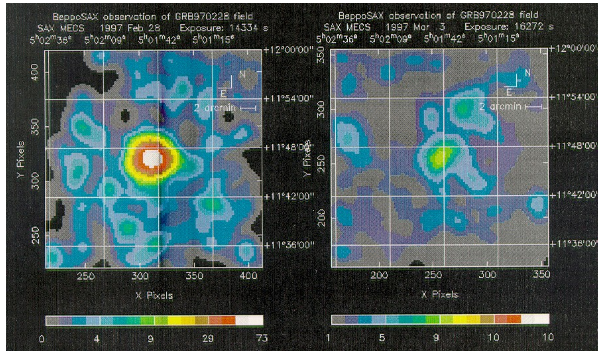

GRB 970228

Costa et al. (1999)

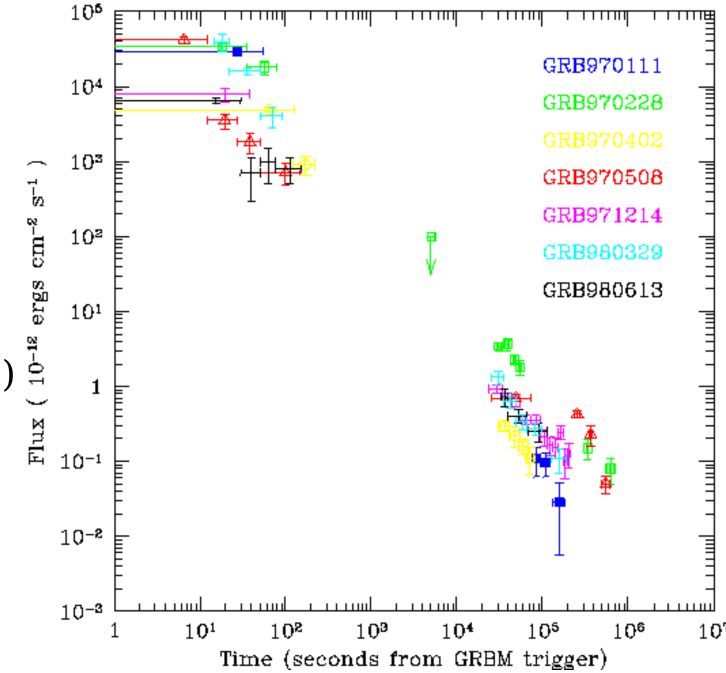

- Beppo-Sax X-ray discovery of fading X-ray afterglows: "all" long-duration GRBs have X-ray afterglows)
  - Sensitivity WFC ~10^{-8} - 10^{-10} ergs cm^{-2} s^{-1}
  - Sensitivity NFI ~10^{-12} - 10^{-14} ergs cm^{-2} s^{-1}
- Power law decay ~$t^{-\chi}$, χ ~ 1.1 - 1.5
- X-ray lines and absorption edges:
  - Fluorescence Fe Kα line
  - Fe absorption feature in prompt phase
  - Variable X-ray absorption (variations in N_H)
- Nonthermal optical: cooling behavior, temporal breaks
  - 1/3 dark bursts
  - Dusty media
  - SFR correction for N_H ~ 10^{22} - 10^{24} cm^{-2}
- Radio ~ 25%, scintillations, SSA, bright early flares
- 17+/- (1-2) GRBs with measured redshifts
- Anomalous(?) GRB 980425 with SN 1998bw

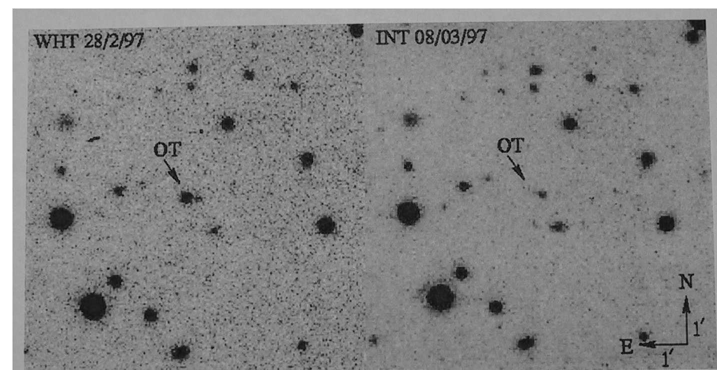

Figure 5 Discovery images of the optical afterglow of GRB 970228 at La Palma (Van Paradijs et al 1997).

GRB/optical transient discovery ima

van Paradijs et al. (1997)

Optical transient discovery image

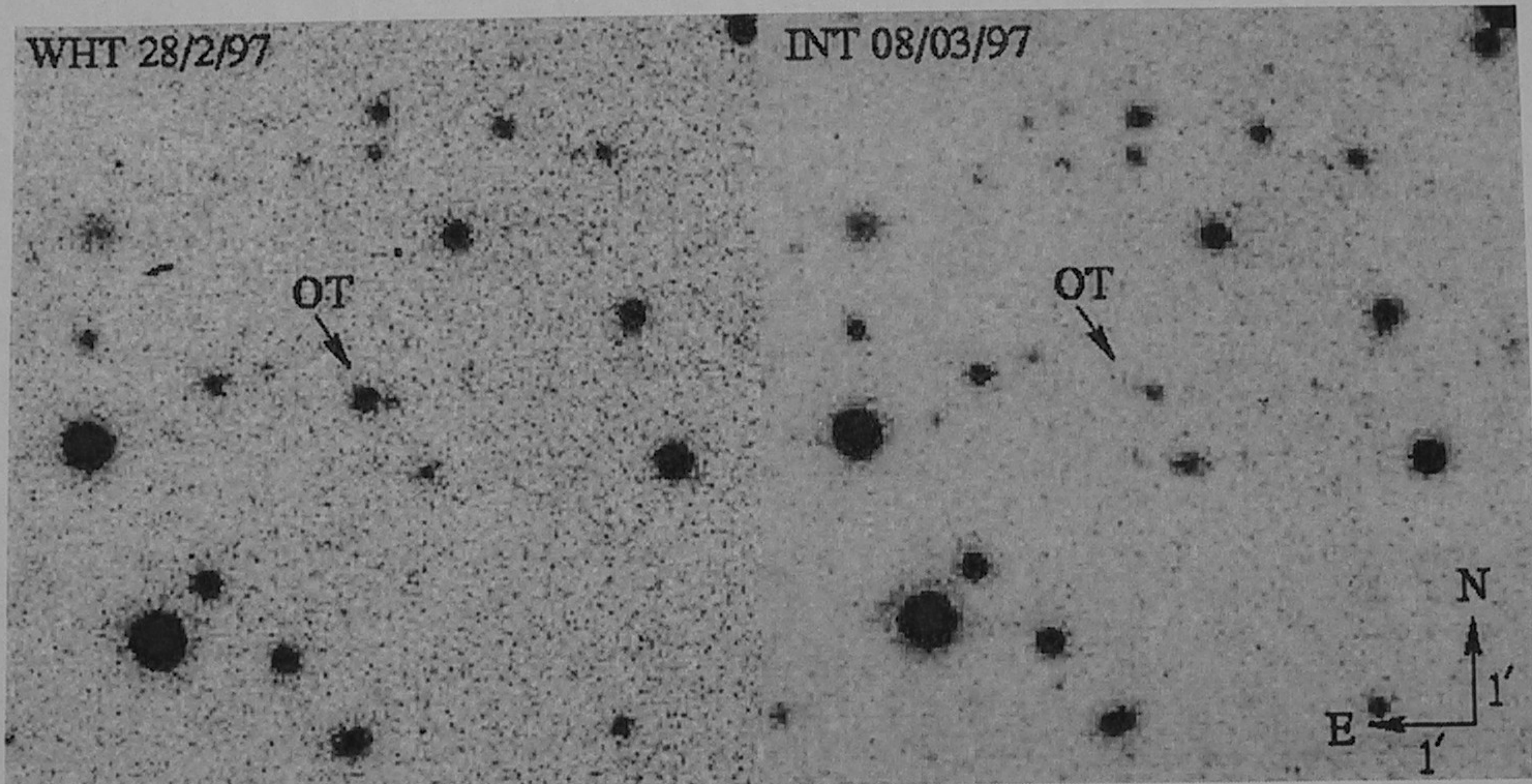

Figure 5 Discovery images of the optical afterglow of GRB 970228 at La Palma (Van Paradijs et al 1997).

Optical spectrum of GRB 970508

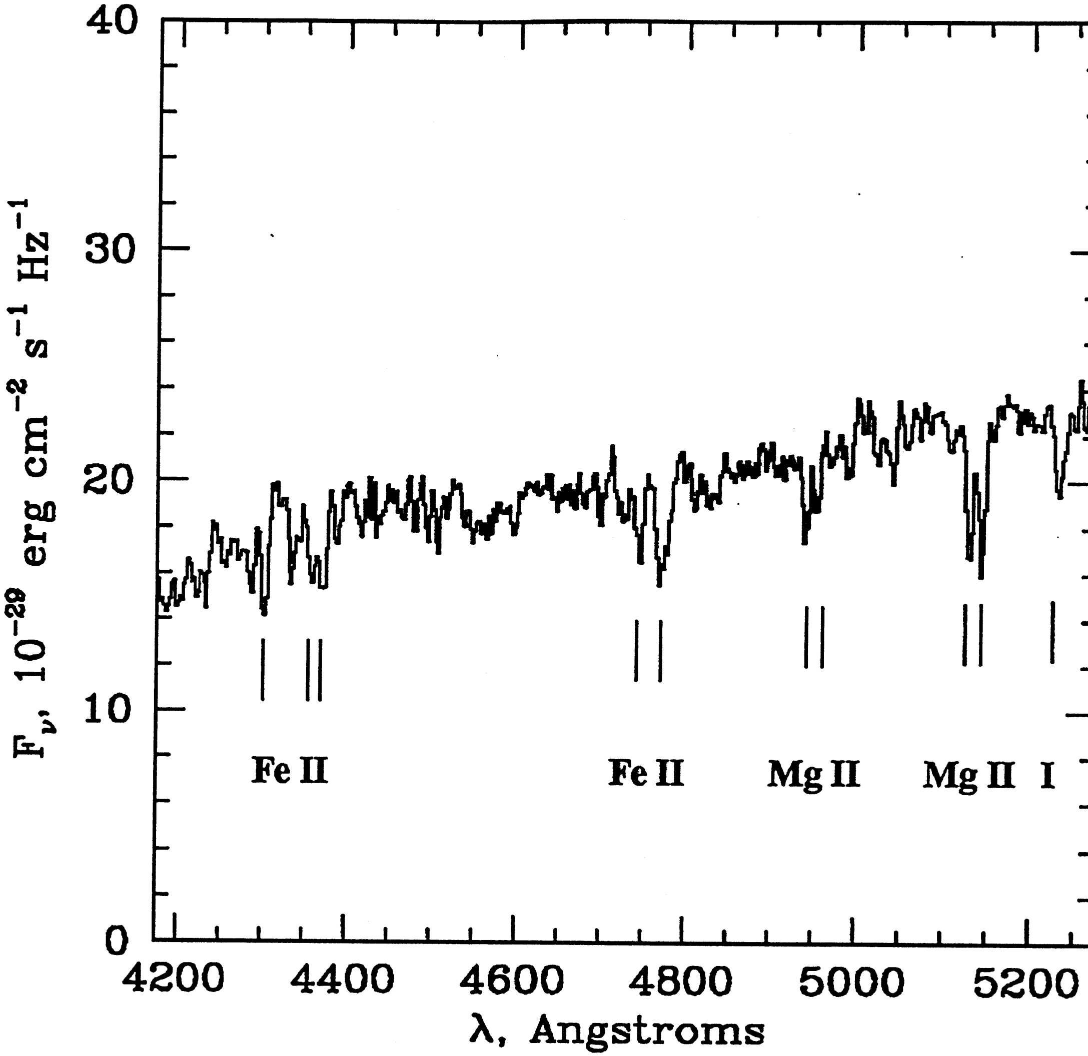

Figure 9 The spectrum of the OT of GRB 970508, showing Fe and Mg absorption lines at z = 0.835 and z = 0.77 (Metzger et al 1997b).

Redshift and Apparent Isotropic Energy Distribution

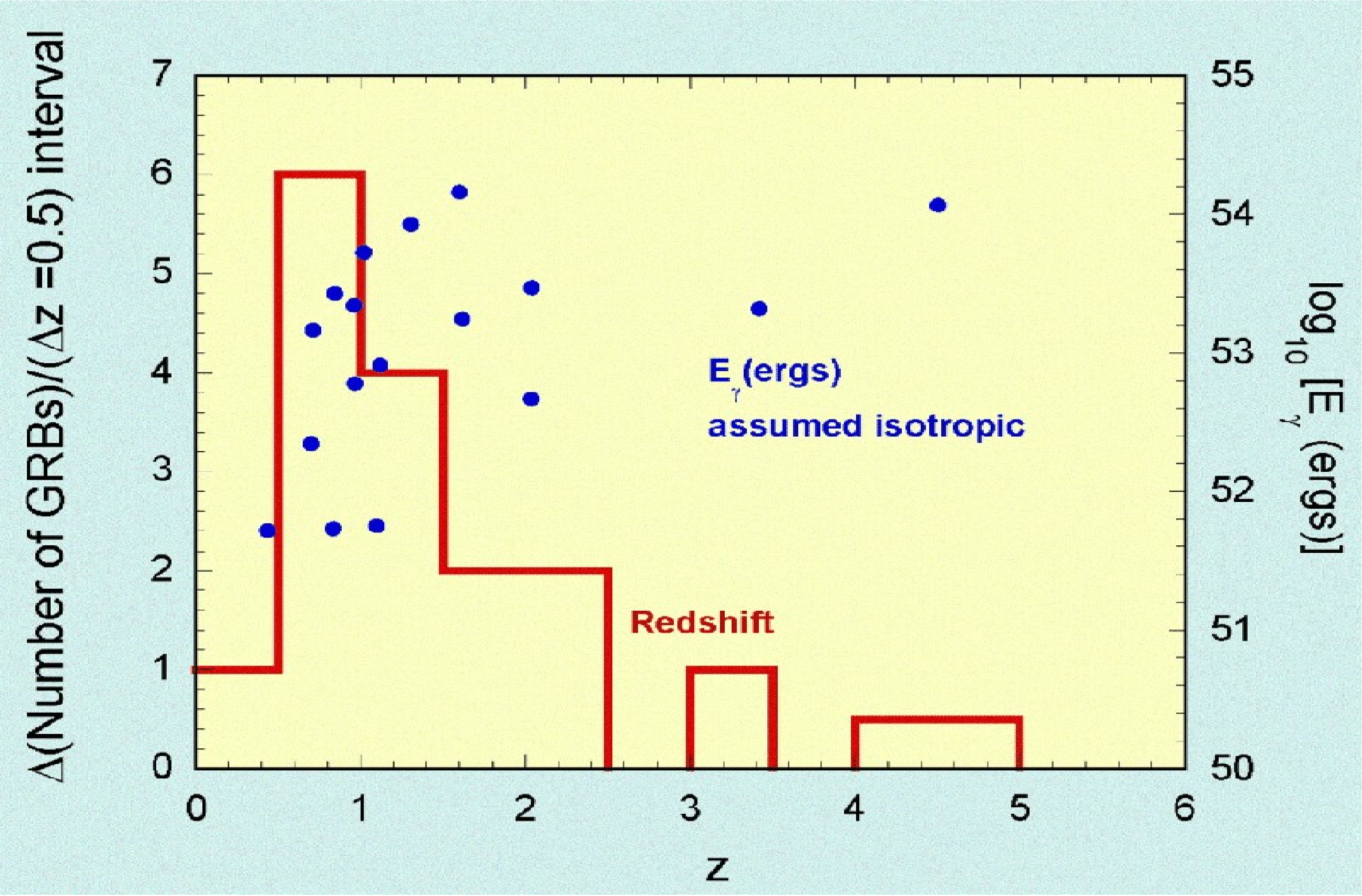

Radio scintillation

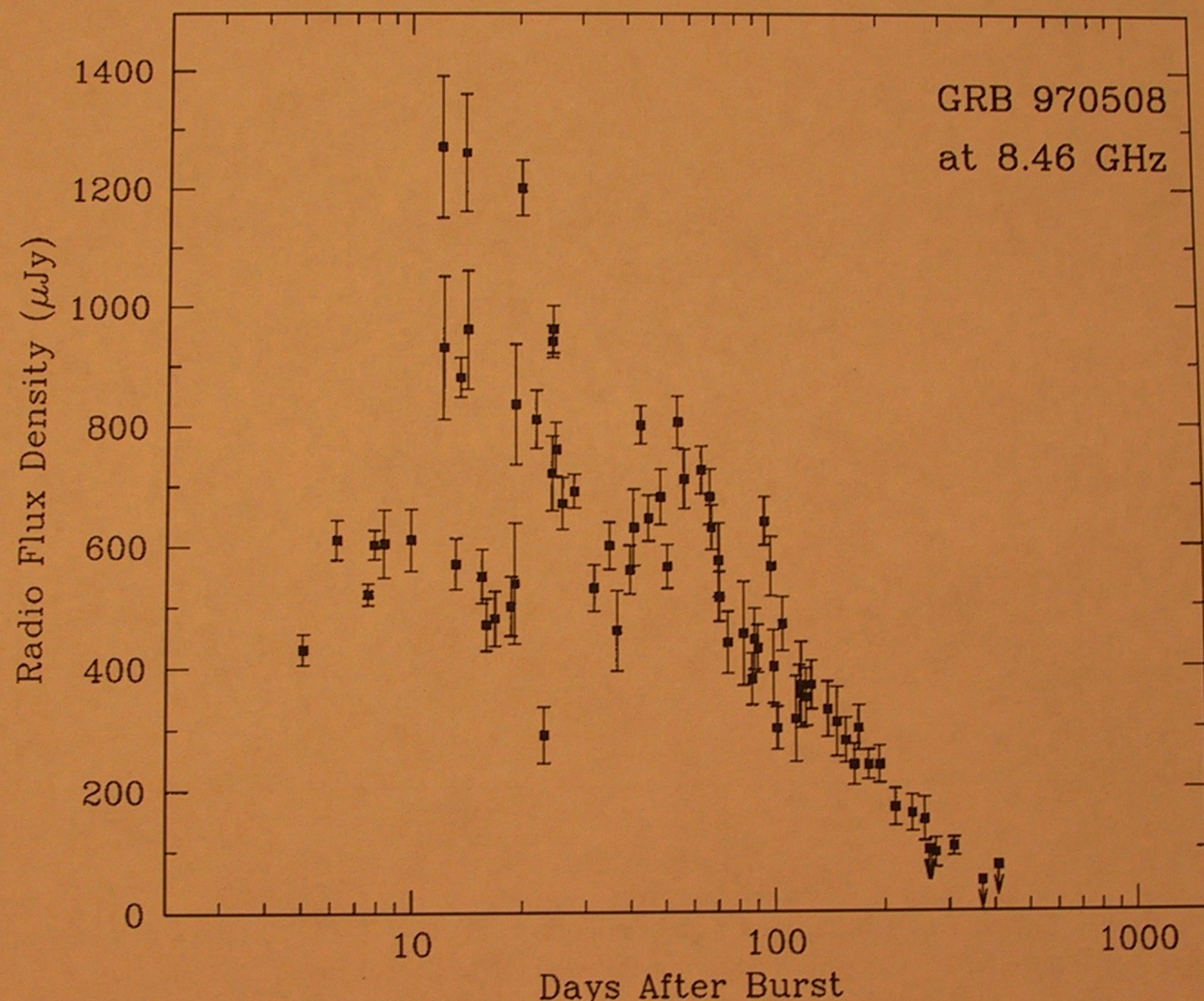

Figure 11 The 8.46 GHZ VLA light curve of the afterglow of GRB 970508 (Kulkarni et al 2000). Note the large scintillation fluctuations in the first month and their later absence, indicating that the source expanded (Frail et al 1997c).

High-energy GRB radiation

1. Origin of hard radiation?
2. Synchrotron
3. SSC
4. Hadronic (synchrotron/photomeson/secondary production)

→ **Nonthermal processes**

Hurley et al. 1994

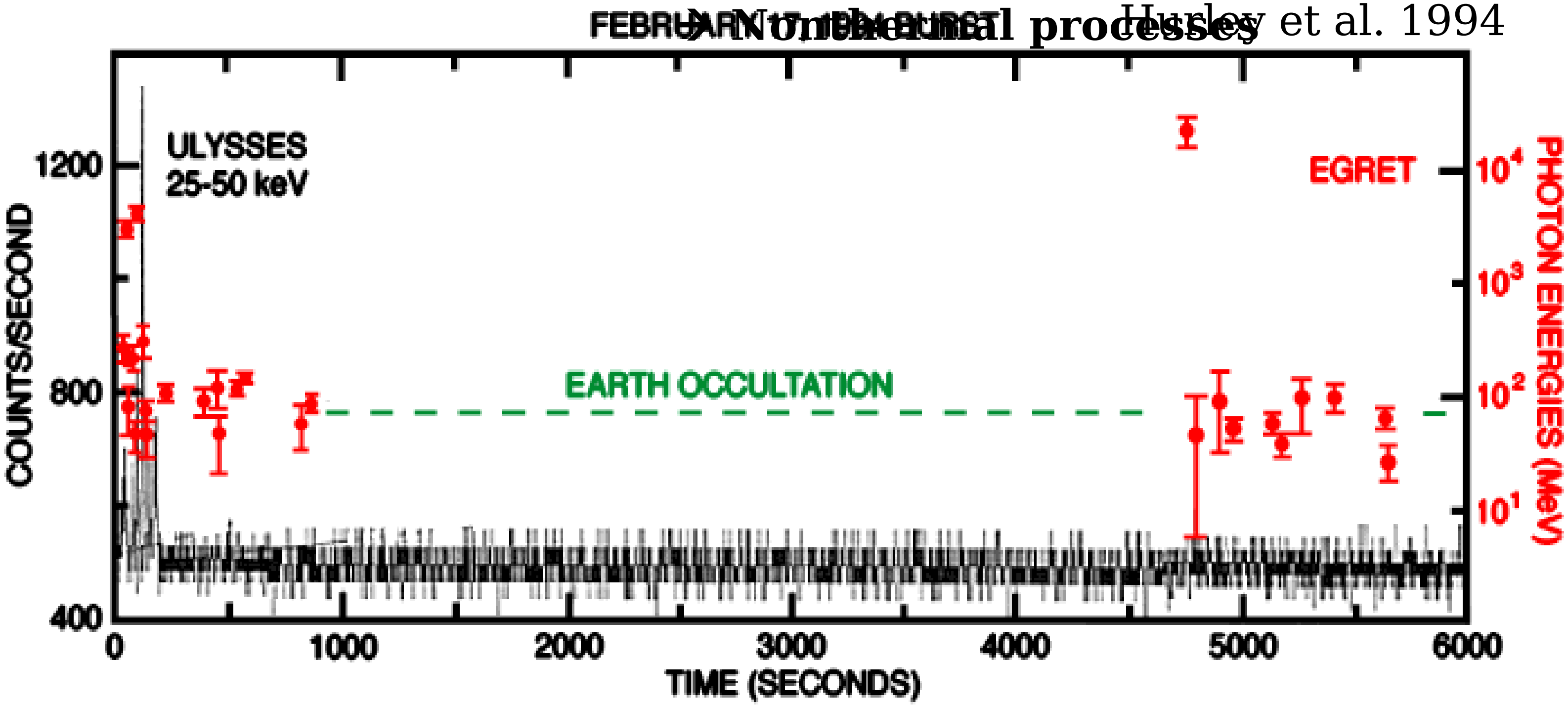

- TeV radiation (Milagrito) Atkins et al. (2000)

Phenomenology

- **BATSE channel lags (Norris et al.) vs. luminosity**
- **Cepheid-like indicator (variability vs. Peak luminosity) (Rameriz-Ruiz, Fenimore et al.)**
- **Hard-to-soft evolution and hardness-intensity correlations in prompt phase**
- **Liang-Kargatis relation govening fluence and E_{pk}**
- **Time dilation**
- **Hardness-duration correlation**
- **Type II XRB behavior in separated pulses (Rameriz-Ruiz and Rees)**
- **Band fits and evolution**
- **Size distributions and cosmological statistics**
- **…**

Cosmological GRB radiation model

- **Cannonball model** (eigine gefahr)

- **Fireball/blast wave model** (Meszaros, Rees, Paczynski, Piran, Waxman, Vietri, Kulkarni, Panaitescu, Kumar, Dai, Lu, Chiang, Böttcher, Lazzati, Dermer, Granot, Katz, Sari, Narayan, and many others)

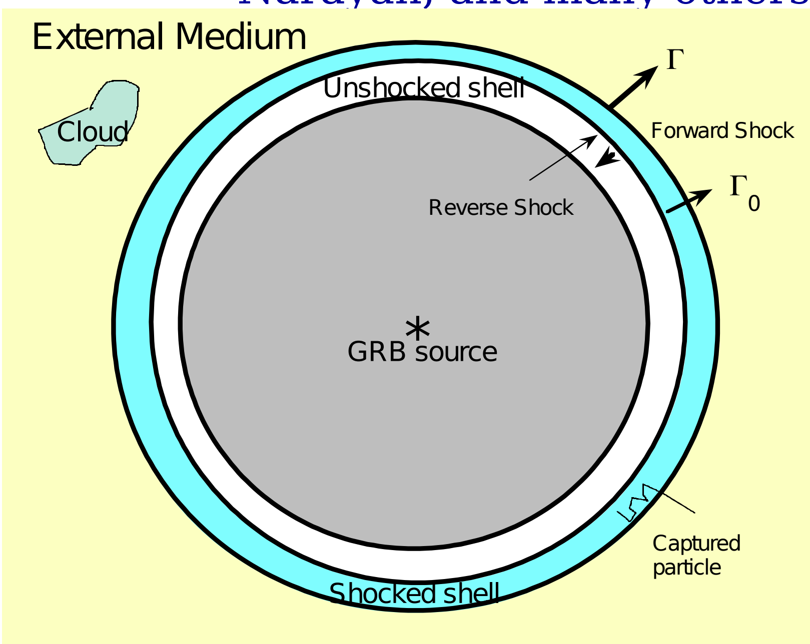

Standard (naïve) blastwave model

1. Spherical, uncollimated explosion
2. Uniform surrounding medium
3. Blast wave approximated as a uniform thin shell
4. Particle acceleration at forward shock only

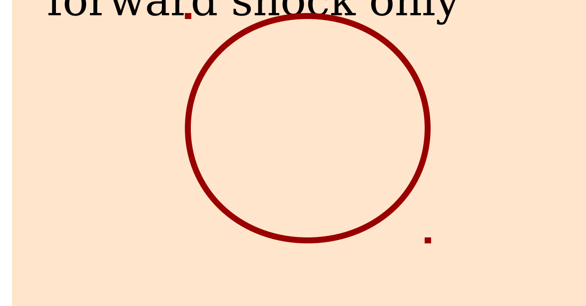

Nonrelativistic reverse shock when $\Gamma < \sqrt{\frac{n'_{sh}}{n_{ISM}}}$

(Sari and Piran 1995)

Geometry of moving systems

Doppler factor: $\delta = [\Gamma(1-\beta\cos\theta)]^{-1}$

Three frames of references:

Director's (God's) frame $\mathbf{dt_*}$

Proper (comoving) frame **dt'**

Observer – that's our – frame **dt**

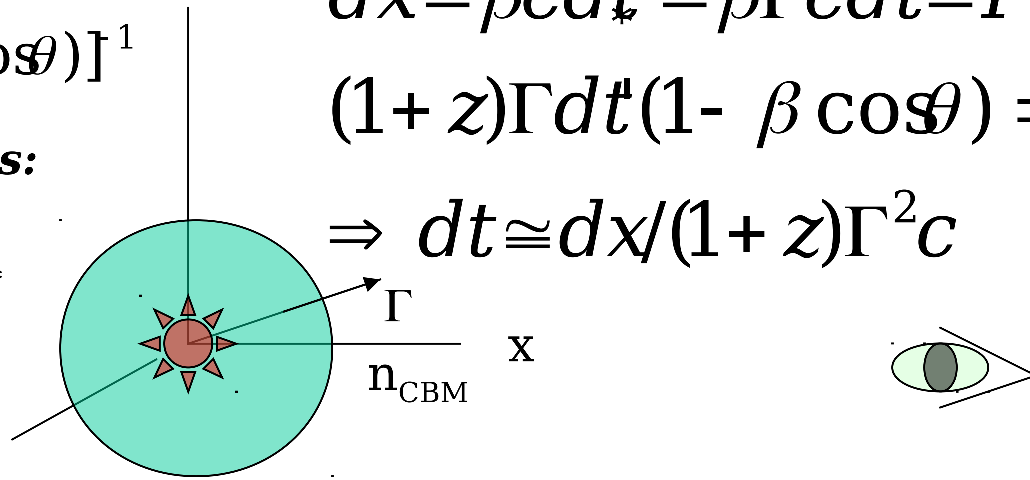

$$dx = \beta c dt_* = \beta\Gamma c dt' = P c dt'$$

$$(1+z)\Gamma dt'(1-\beta\cos\theta) = dt$$

$$\Rightarrow dt \cong dx/(1+z)\Gamma^2 c$$

$$E = \delta E'/(1+z) \cong \Gamma E'/(1+z)$$

$$E_* = \Gamma E'; dt_* = \Gamma dt'$$

$$dE_*/dt_* = dE/dt' = 4\pi n_* m_p c^3 \beta x^2 (\Gamma^2 - \Gamma)$$

$$\Gamma^2 - \Gamma \to \beta^2/2, nonrelativistic$$

$$\Gamma^2 - \Gamma \to \Gamma^2, relativistic$$

Blandford and McKee (1976)

Spherical blast-wave evolution in adiabatic regime

$$\Gamma[M_0+\Gamma m_{su}(x)]=\Gamma[M_0+k\Gamma x^3]=cons$$

$$\Rightarrow\ \Gamma\propto x^{-3/2}$$

Blast wave momentum P = βΓ

Initial blast wave momentum $P_o = \beta_o\Gamma_o$

Internal kinetic energy U

$$-\frac{dP}{dx}=\frac{P\Gamma(dm/dx)+(\Gamma^2/P)(dU_{adi}/dx)}{M_0+m(x)+U}$$

$$U=m_p\int_0^\infty dp'(\gamma'-1)N'(p';x)$$

$$\boxed{P(x)=\frac{P_0}{\sqrt{1+(x/x_d)^3}}}$$

Dermer and Humi (2001)

$$\frac{dp'}{dx}\Big|_{adi}=-p'\left(\frac{1}{x}-\frac{1}{3}\frac{d\ln\Gamma}{dx}\right)$$

Deceleration radius

$$x_d=\left(\frac{3E_0}{4\pi m_p c^2 n_*\Gamma_0^2}\right)^{1/3}$$

$$=2.6\times10^{16}\left(\frac{E_{52}}{n_*\Gamma_{300}^2}\right)^{2/3}cm$$

Deceleration time

$$t_d=\frac{x_d}{P_0\Gamma_0 c}$$

$$\cong\frac{10}{\beta_0}\left(\frac{E_{52}}{n_*\Gamma_{300}^8}\right)^{2/3}s$$

Recover Sedov solution

when $P_0\rightarrow\beta_0$

$$v(x)\propto x^{-3/2}$$

$$x\propto vt\Rightarrow\ x\propto t^{2/5},v\propto t^{-3/5}$$

Relativistic (Γ>>1) behavio[r]

$$\Gamma\propto x^{-3/2}$$

$$t\cong c^{-1}\int dx/\Gamma^2\propto\int dx\,x^3$$

$$\therefore\ x\propto t^{1/4},\Gamma\propto t^{-3/8}$$

Adiabatic Blast Wave Evolution

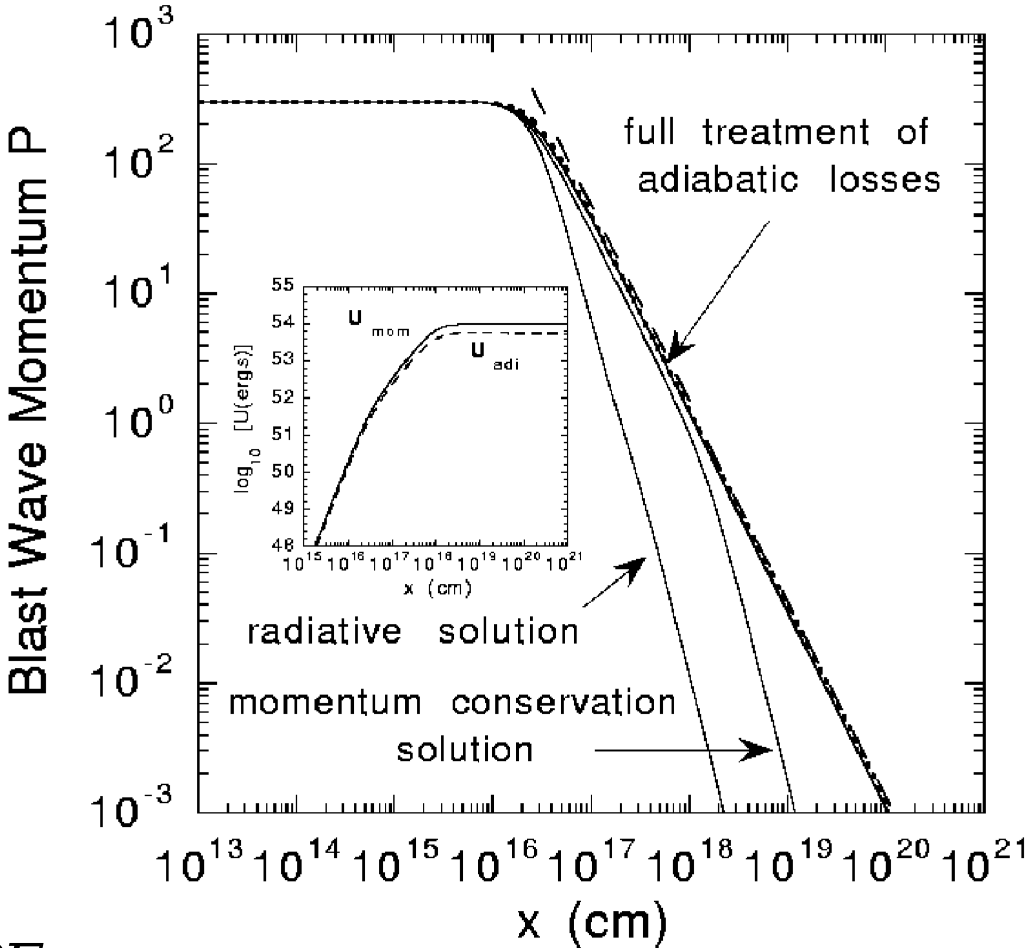

Sedov length:

$$\ell_S = \Gamma_0^{\,2} x_d = \left(\frac{3E_0}{4\pi m_p c^2 n_*}\right)^{1/3} \approx 2.1 \left(\frac{m_0}{n_*}\right)^{1/3} pc$$

Sedov age:

$$t_S = \ell_S / v_o \approx 2 \times 10^{10} \left(\frac{m_0}{n_*}\right)^{1/3} \left(\frac{v_o}{0.01c}\right)^{-1} s$$

Elementary Blast Wave Theory

- Nonthermal synchrotron radiation in shocked fluid
  - Joint normalization to power and number gives

$$\gamma_{\min} \cong \epsilon_e \left(\frac{p-2}{p-1}\right)\left(\frac{m_p}{m_e}\right)\Gamma \; ; \; \dot{E}'_e = \epsilon_e (dE'/dt')$$

- Magnetic field parametrized in terms of equipartition field

$$\frac{B^2}{8\pi} \cong 4\epsilon_B m_p c^2 n_* (\Gamma^2 - \Gamma) \Rightarrow B \propto \Gamma$$

- Injection of power-law electrons downstream of forward shock

$$N(\gamma_e) = N_e \gamma_e^{-p}, \; \gamma_{\min} < \gamma_e < \gamma_2 \; (comoving\ \gamma_e)$$

$$N_e = 4\pi\, n_{ext} x^3/3$$

- Maximum injection energy: balancing losses and acceleration rate

$$\gamma_2 \cong 4\times 10^7/\sqrt{B(G)}$$

- Cooling electron break: balance synchrotron loss time with adiabatic expansion time

$$t'_{adi} \cong x/\Gamma c \cong \Gamma t \cong t'_c \cong \left(\frac{4}{3} c\sigma_T \frac{u_B}{m_e c^2}\gamma_c\right)^{-1}$$

$$\Rightarrow \gamma_c \cong \frac{3m_e}{16\epsilon_B n_* m_p c\sigma_T \Gamma^3 t} \;\Rightarrow\; \gamma_{\min} \propto t^{-3/8}, \gamma_c \propto t^{1/8}$$

The difference between a blob and a blast wave

1. Blob

$$r_b = \frac{c\delta t_{var}}{1+z} \qquad (1+z)\Gamma\Delta t'(1-\beta_\Gamma\mu) = \Delta t$$

$$f_\epsilon^{syn} = \frac{\delta^4}{4\pi d_L^2}\epsilon' L_{syn}(\epsilon') \cong \frac{\delta^4}{4\pi d_L^2}\left[\frac{1}{2}u_B c\sigma_T \gamma^3 N_e(\gamma)\right]$$

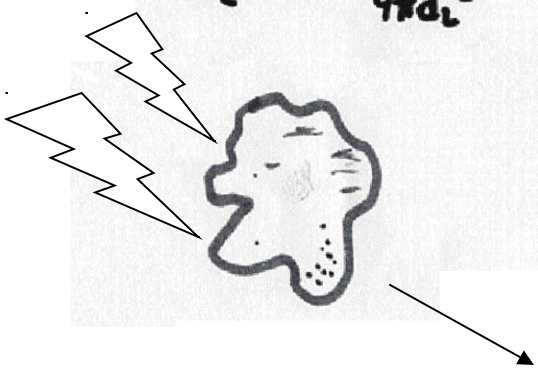

$$\gamma = \sqrt{\frac{(1+z)\epsilon}{\delta\epsilon_B}}$$

Blob: 4 powers of Doppler factor δ; 2 from solid angle, 1 from energy and 1 from time

2. Blast Wave

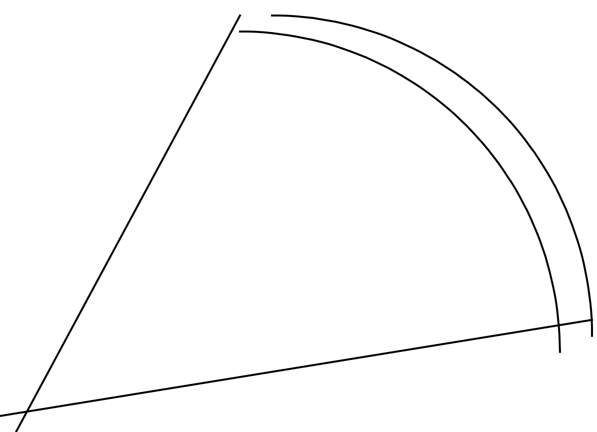

In the beam

$$\theta < \Gamma^{-1}$$

$$f_\varepsilon \approx \frac{\Gamma^2 \varepsilon' L_{syn}(\varepsilon')}{4\pi d_L^2 (1+z)^2}$$

Blast wave: 2 powers of δ~Γ; 1 from energy and 1 from time

Lateral expansion of shell
(Rhoads and Paczynski)

Transition from fast to slow cooling – if parameters e_e, e_B, p stay constant

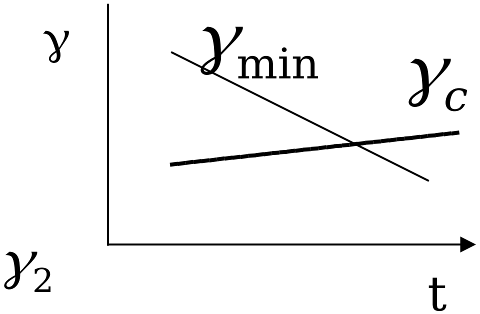

Comoving Nontherm al Electron Spectrum

$$N_e(\gamma_e) \cong N_e \gamma_o^{s-1}\gamma_e^{-s}, \quad \gamma_0 < \gamma_e < \gamma_1$$

$$N_e(\gamma_e) \cong N_e^o \gamma_o^{s-1}\gamma_1^{-s}(\gamma_e/\gamma_1)^{-(p+1)}, \quad \gamma_1 < \gamma_e < \gamma_2$$

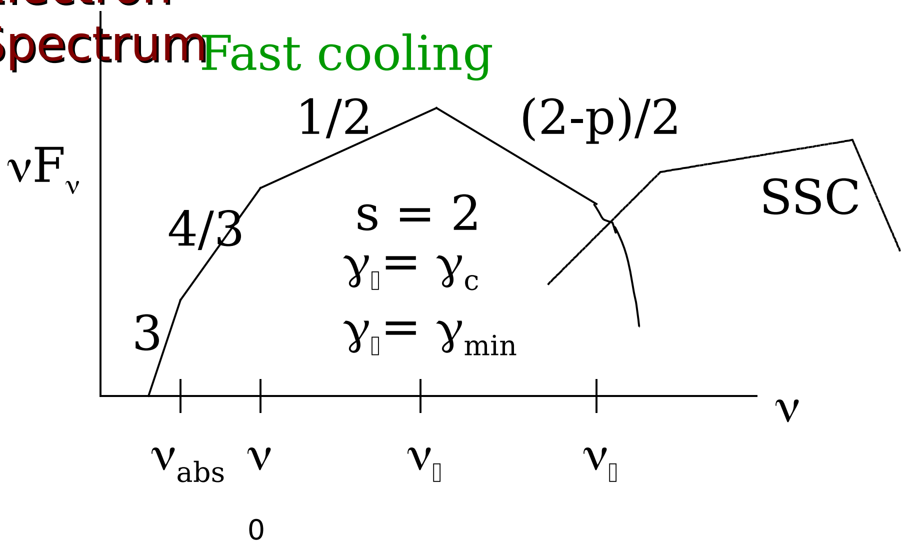

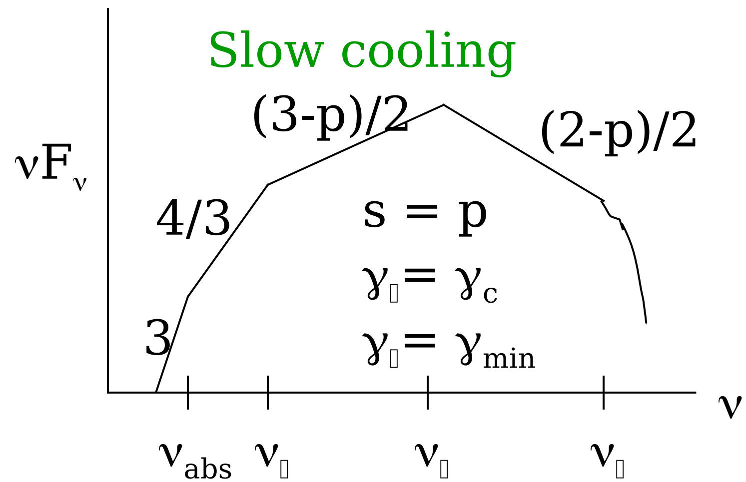

- p > 2
- SSC important when $e_B << e_e$
- Uniform (not wind) geometry

$$\nu_i = \Gamma \gamma_i^2 eB/[2\pi m_e c(1+z)]$$

L_ν Spectrum

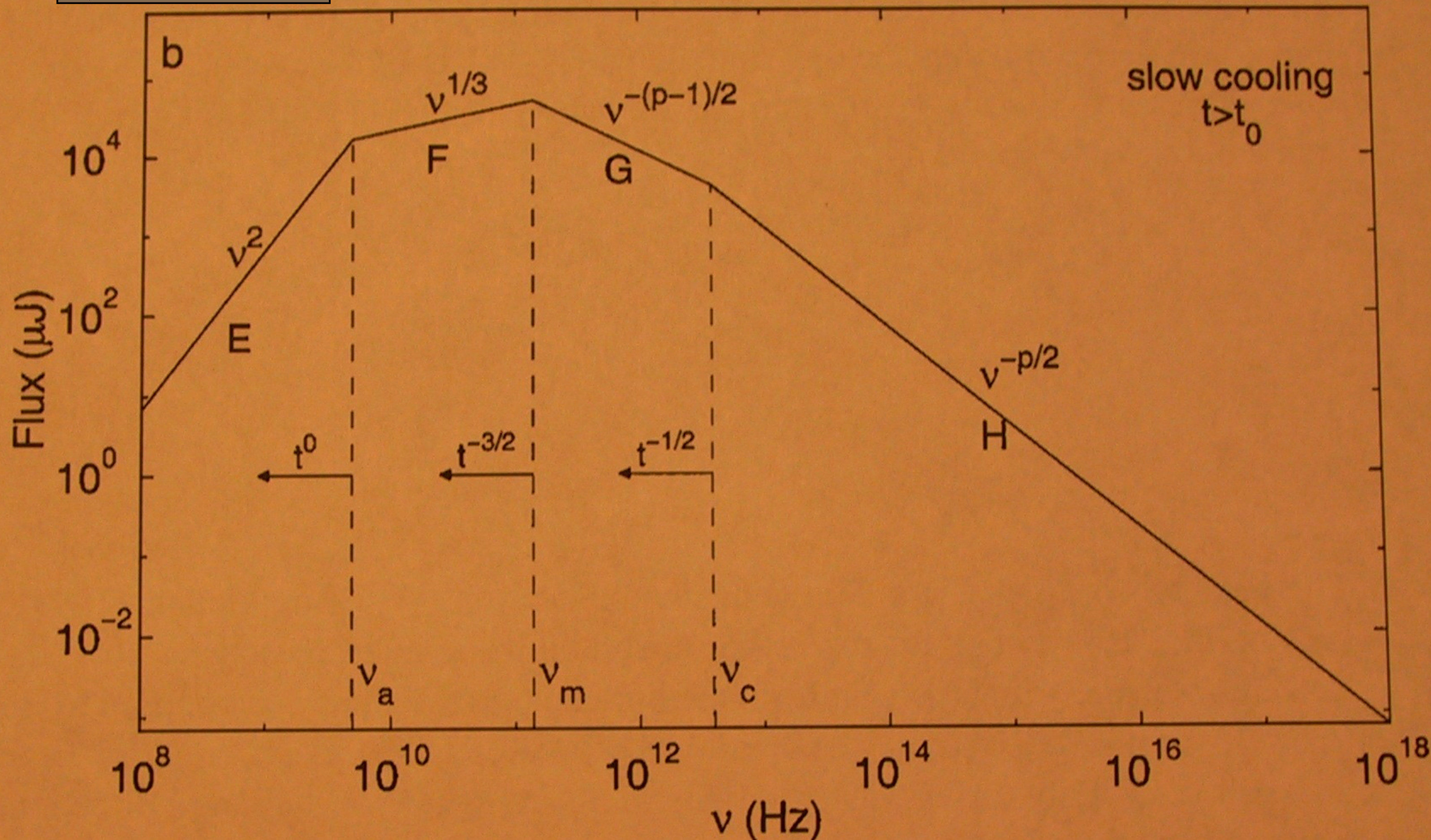

Figure 3 The piecewise power-law schematic shape of blast wave synchrotron spectra for later afterglow evolution (Sari et al 1998). The characteristic break frequencies and their time evolution are indicated, as is the spectral slope in each regime. This can be directly compared with the observed spectrum of GRB 970508 (Figure 12).

GRB 970228 X-ray afterglow

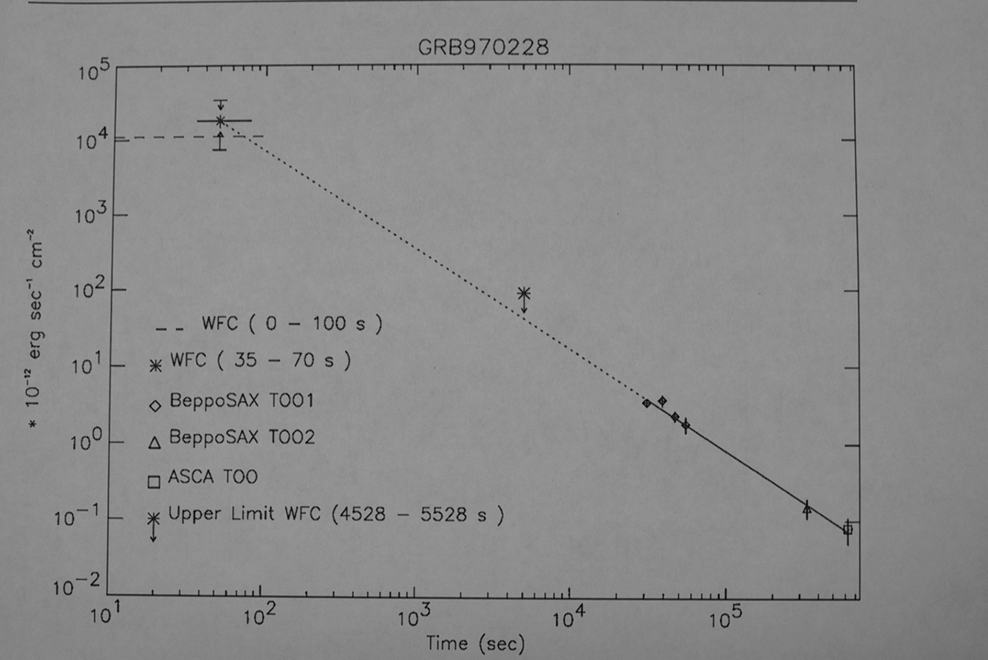

Figure 8 The X-ray afterglow light curve of GRB 970228. Note the smooth connection of the afterglow with the prompt X-ray flux from the GRB (Costa et al 1997b).

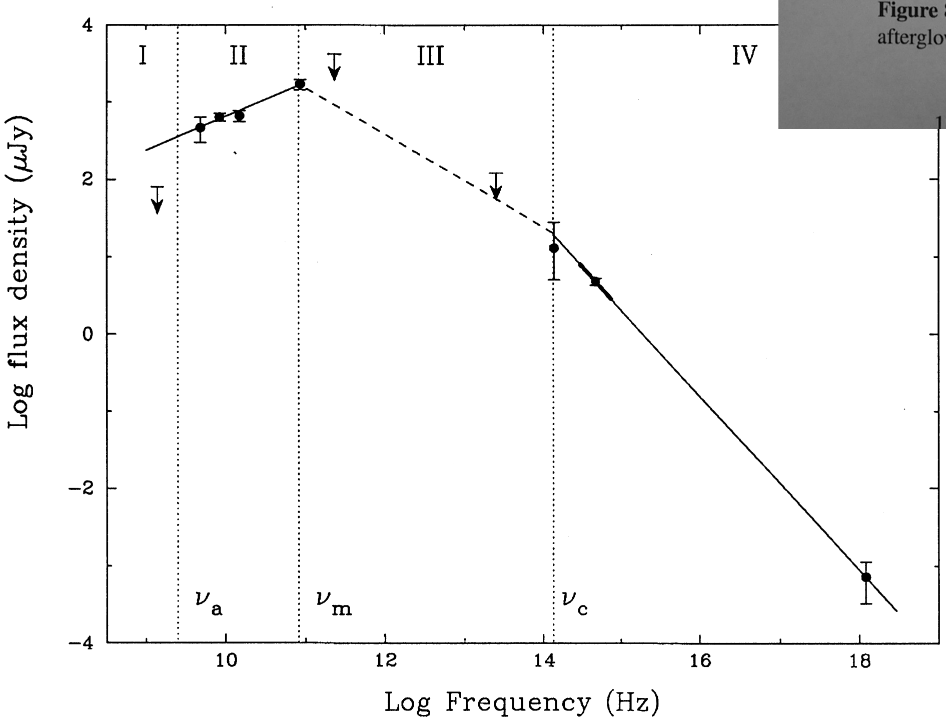

Fit to GRB 9970508

(Wijers and Galama 1999)

Temporal indices

High frequency adiabatic:

1/6; -1/4; (2-2p)/4; (2-3p)/4

Low frequency adiabatic:

1/6; 1/2; 3(1-p)/4; (2-3p)/4

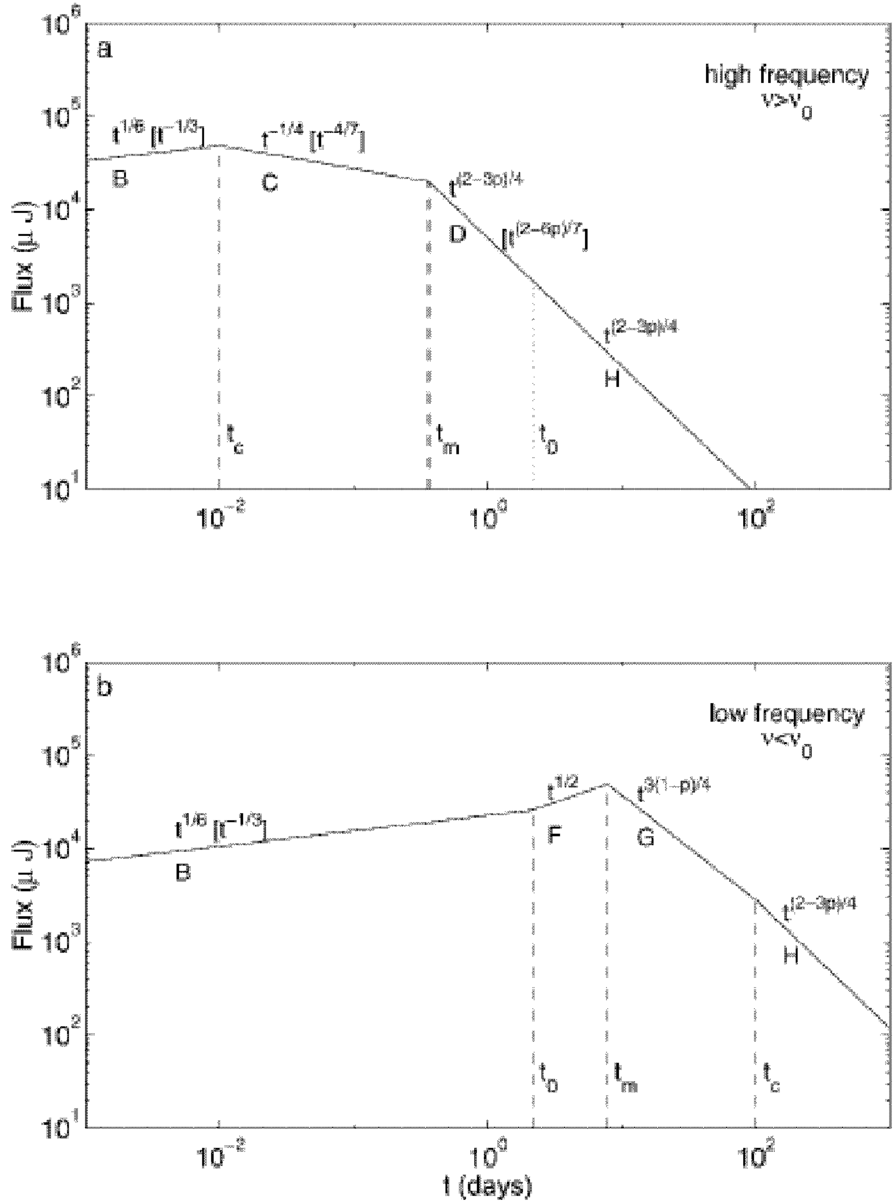

FIG. 2.—Synchrotron light curve (ignoring self-absorption). (*a*) High-

Cooling Spectral Behavior

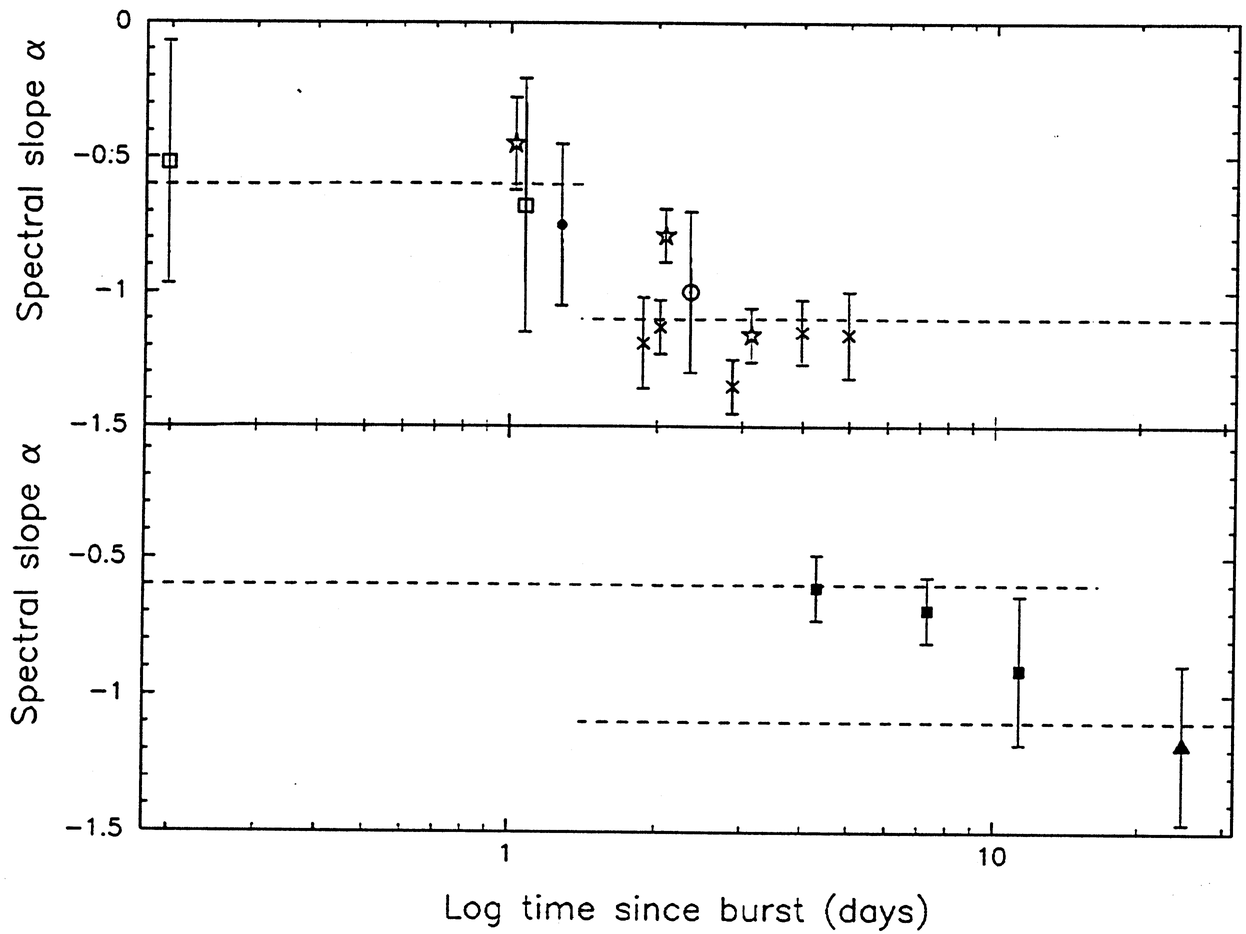

Most common prompt GRB light curve

- Reproduces generic temporal behavior of FRED-type profiles
- Synchrotron-shock model reproduces time-averaged gamma-ray spectra of GRBs (Tavani 1996; Cohen et al. 1997)

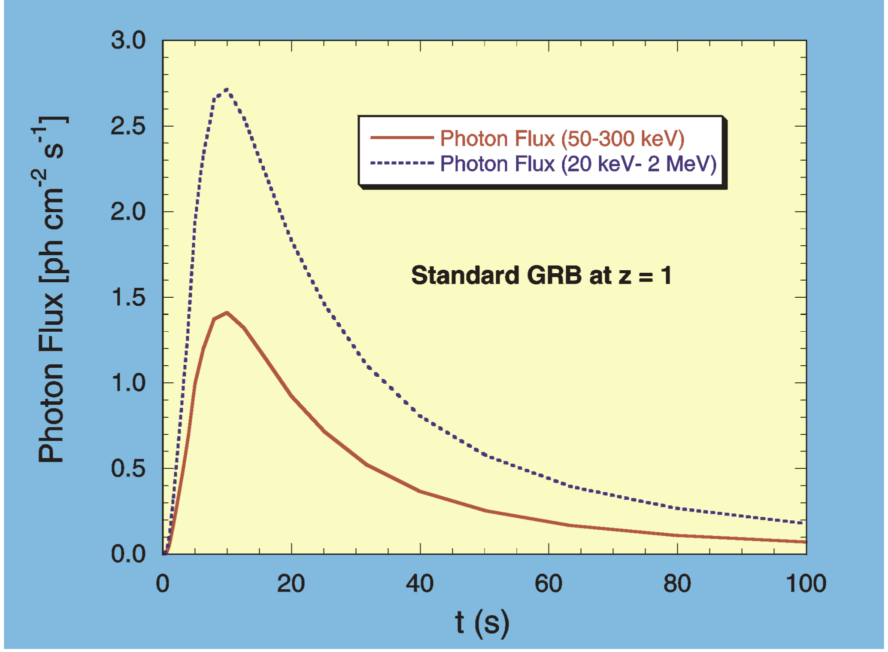

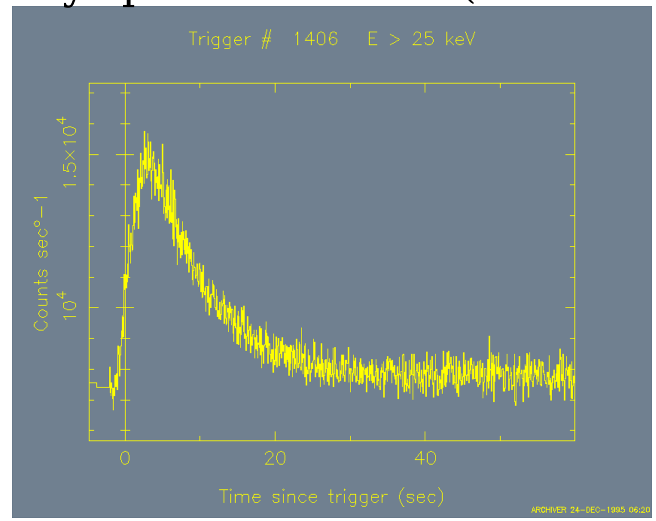

1. Alignment at high energies; lag at lower energies
2. Predictable sequence of energy-dependent temporal indices in rising phase
3. Change in spectral indices between leading and trailing edges of GRB peak follow a well-defined behavior

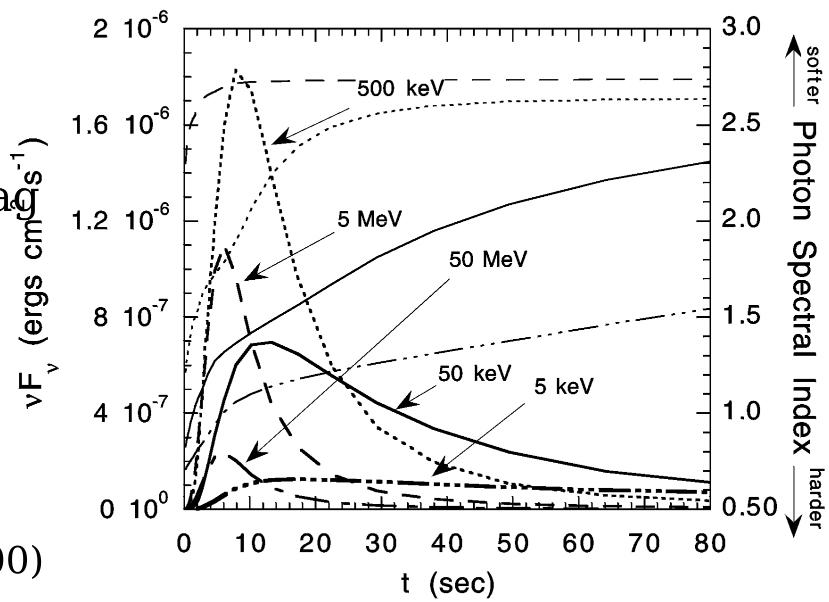

Dermer, Böttcher, and Chiang (2000)

Blast wave model: comparison with numerical simulation results

νF_ν spectra shown at observer times 10^i seconds after GRB event

Panel a: Parameters to fit prompt emission

Panel b: Parameters for afterglow (Wijers and Galama 1999) for

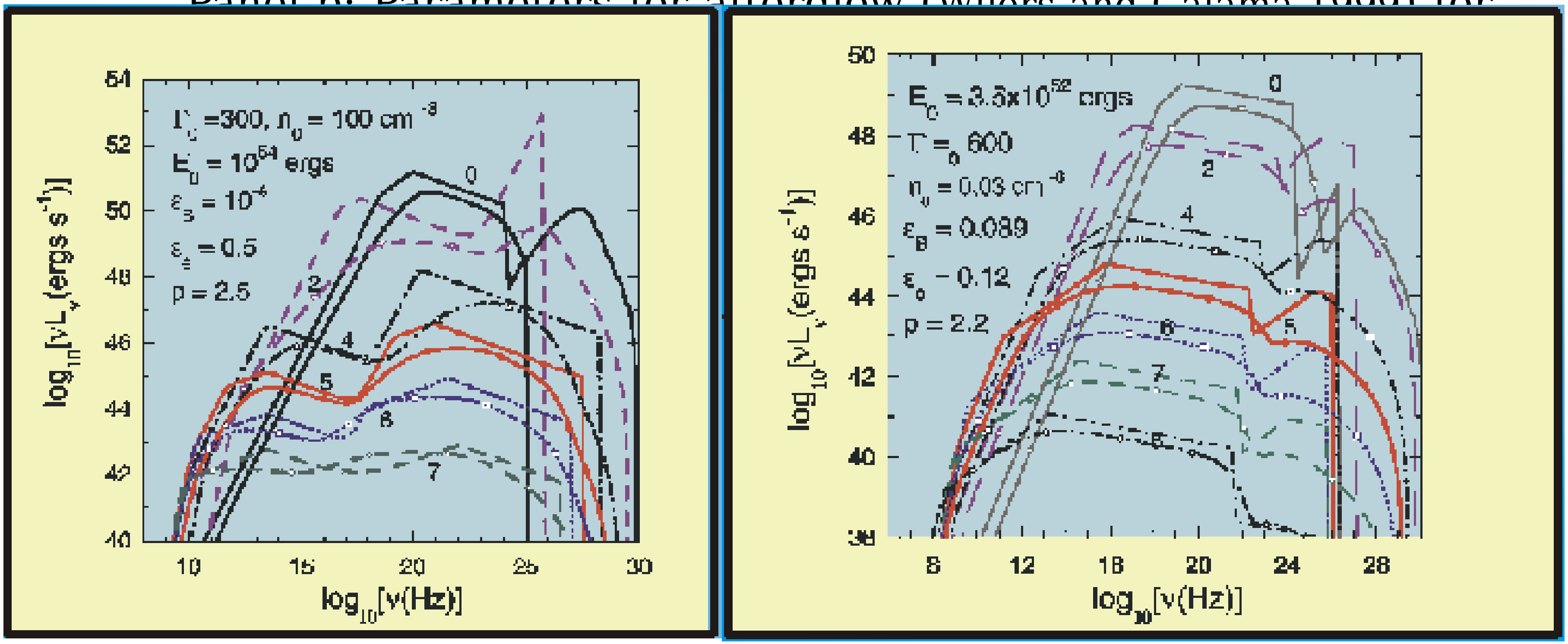

Dermer, Chiang, and Böttcher (2000)

Blast wave model: comparison with numerical simulation results

L_ν light curves and snapshot spectra using parameters for afterglow (Wijers and Galama 1999) of GRB 970508

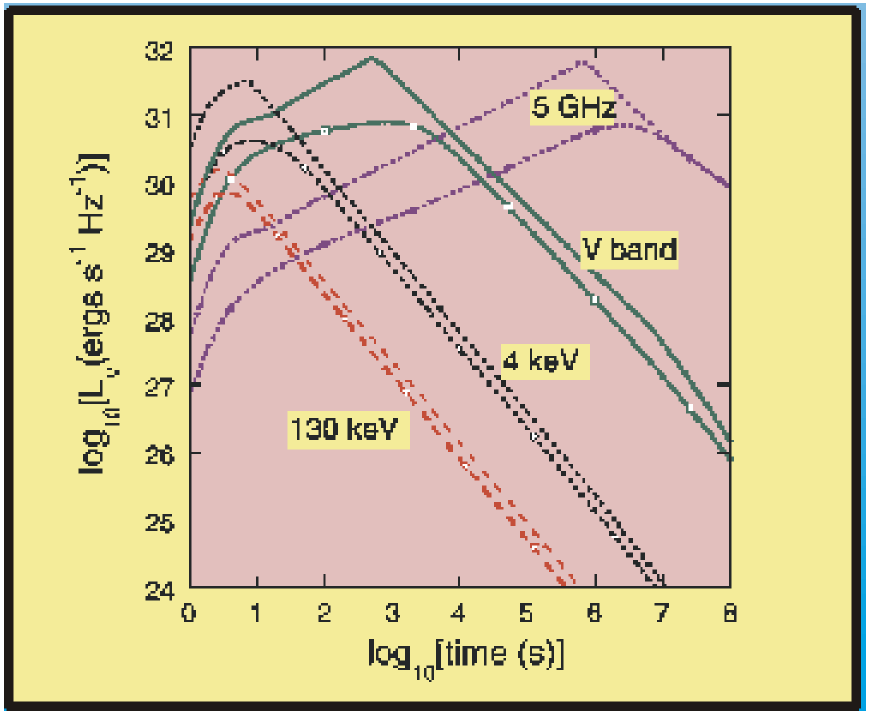

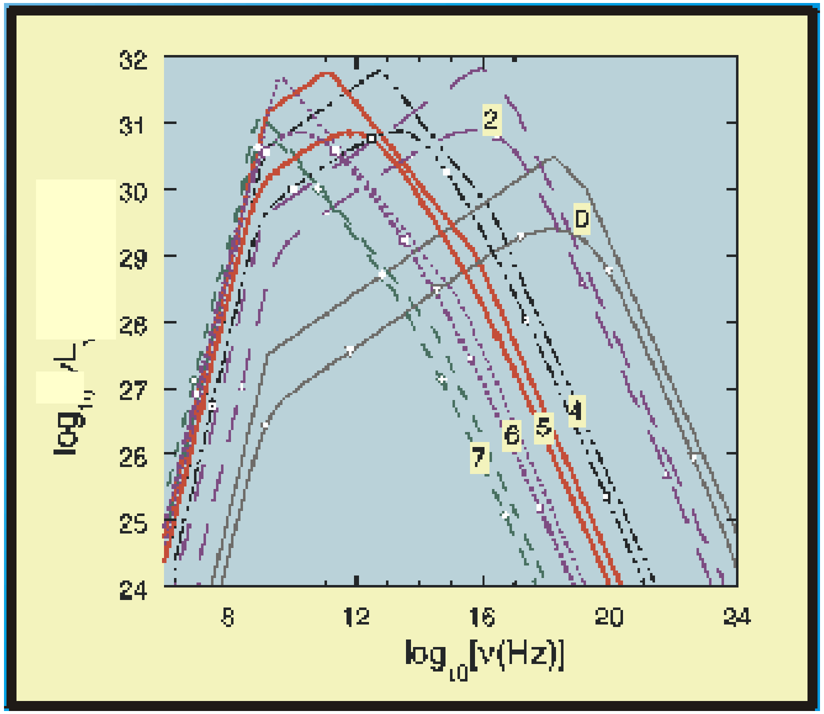

Dermer, Chiang, and Böttcher (2000)

Dirty and Clean Fireballs: strong GeV/TeV sources

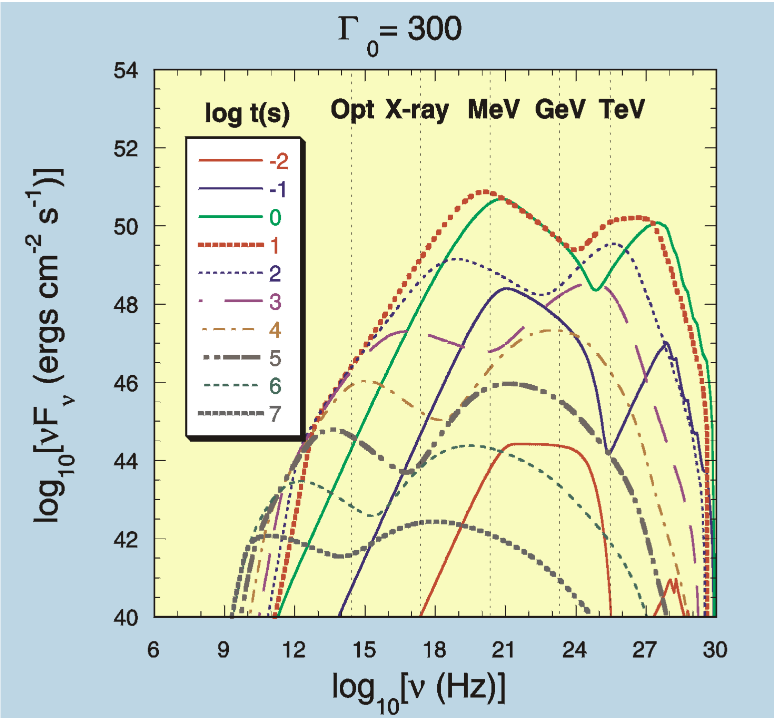

Severe instrumental selection biases against detecting fireballs with Γ_0 << 100 and Γ_0 >> 1000

Lobster-eye telescope to discover dirty fireball transients

GLAST; rapid response ground-based air Chernekov; all-sky water Cherenkov detectors for clean fireballs

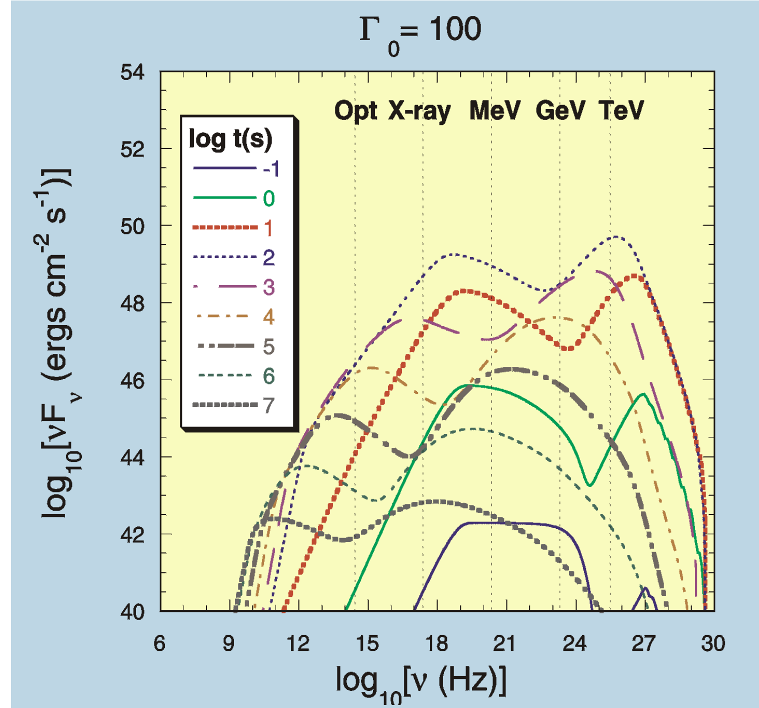

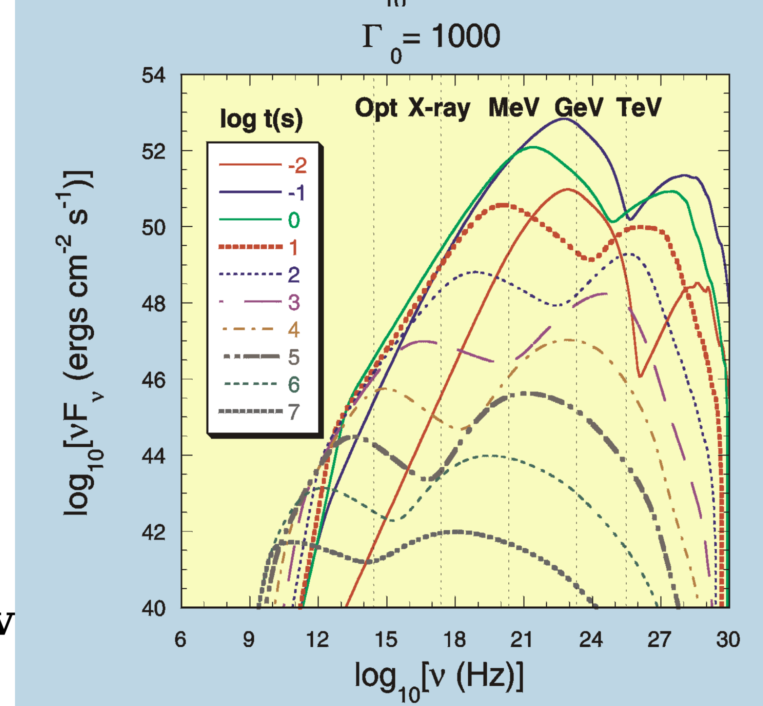

Predicted high-energy behavior in the external shock model

SSC feature seen also at X-ray, optical frequencies

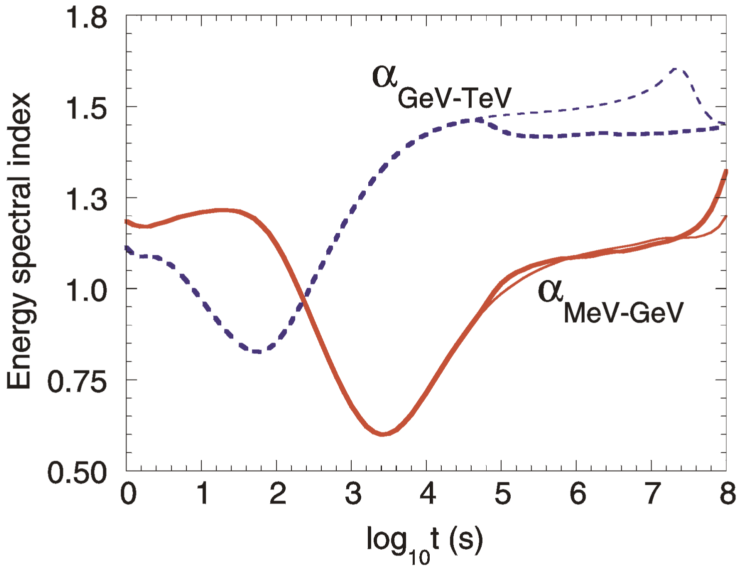

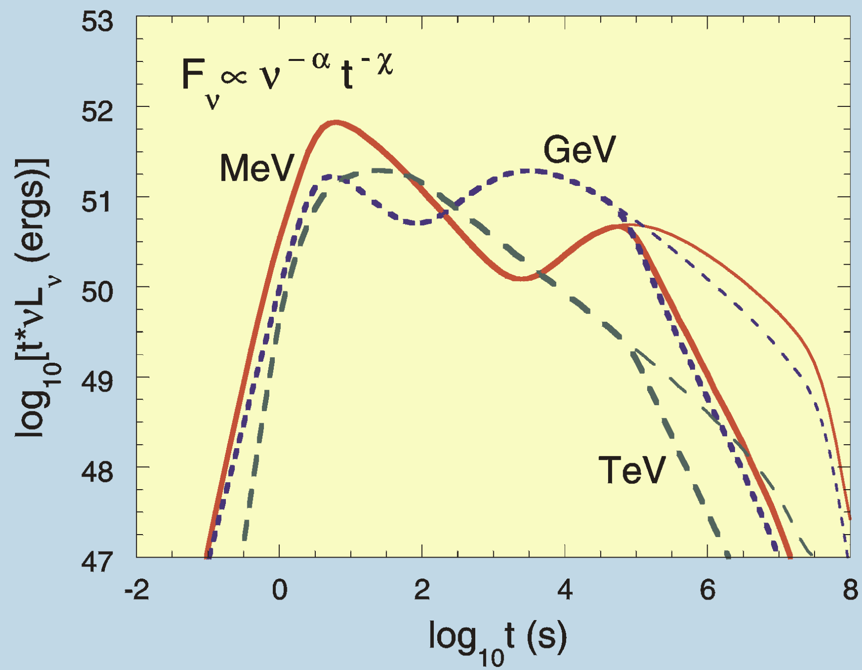

Detailed multiwavelength afterglow modeling

Analysis of 4 GRBs (Panaitescu and Kumar 2001): GRB 980703, GRB 990123, GRB 990510, GRB 991216

with other observations imply

More consistent with uniform surroundings than wind

Moderate magnetic field parameter (e_B ~ 10^{-4} – 0.05); 0.01 <~ e_e <~ 0.1; **θ ~ 1°-4° : beaming factor = 13,000/ (θ °)²**

Implied low density of surroundings (n_{ISM} ~ 10^{-4} – 10 cm^{-3})

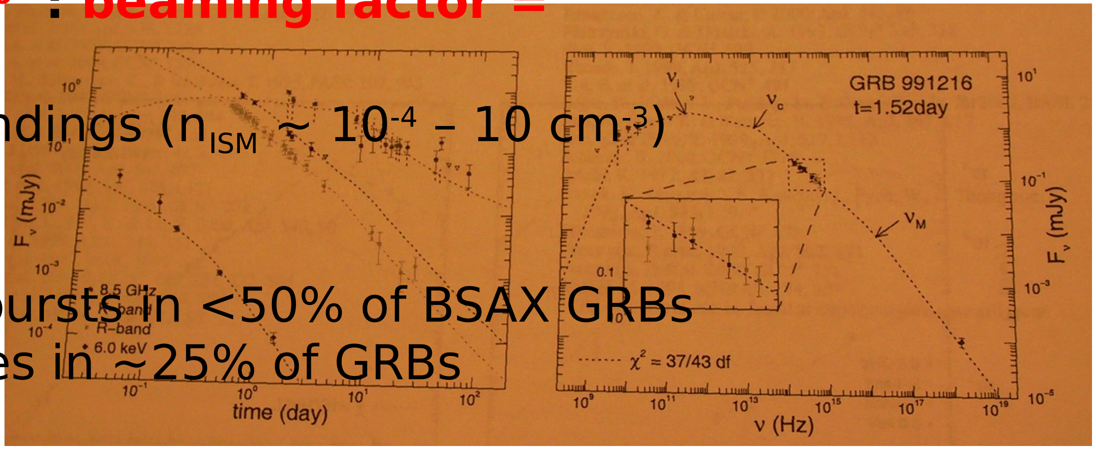

Existence of (optically) dark bursts in <50% of BSAX GRBs

Radio flares on day time scales in ~25% of GRBs (Djorgovski + astro-ph/0107539)

Early (day timescale) radio flares

Numerical light curve and beaming calculations

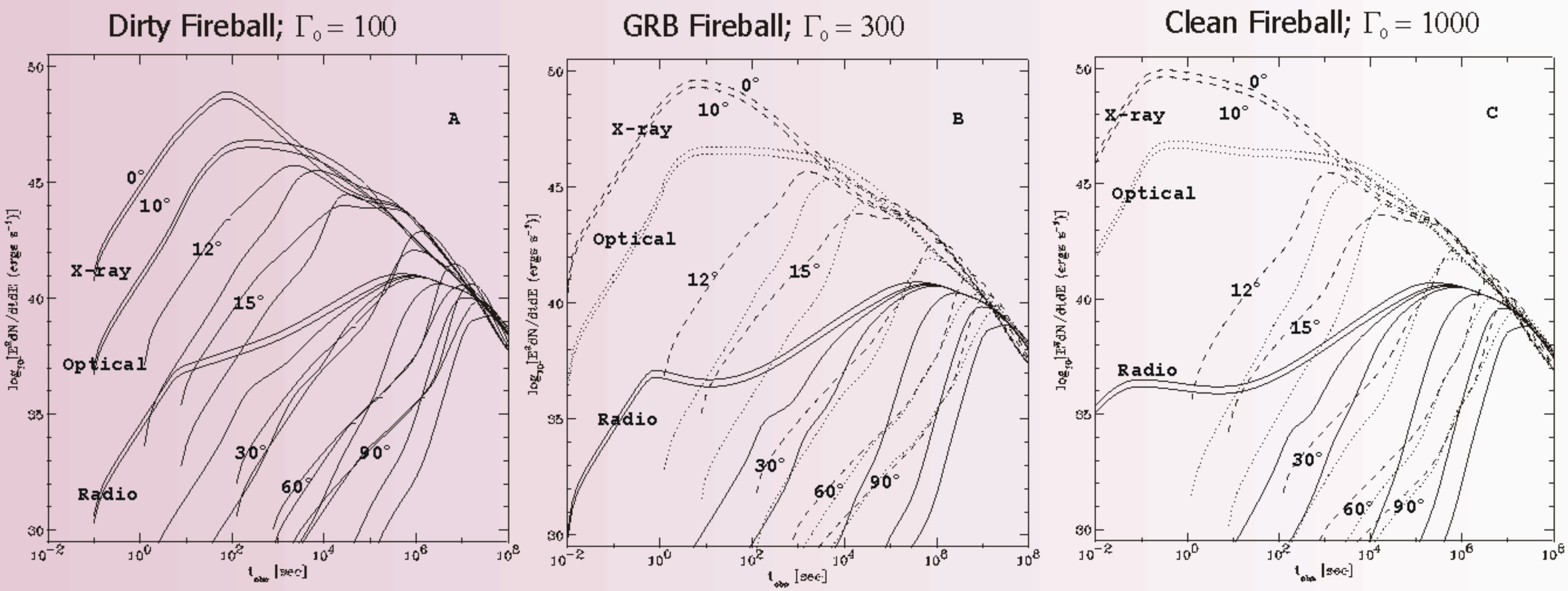

Light curves calculated at various observing energies and inclination angles θ for a fireball blast wave with a standard parameter set and opening half-angle ψ = 10° of the jet. The initial blast wave Lorentz factor Γ_0 = 100, 300, and 1000 in panels A, B, and C. Calculations of θ = 0°, 10°, 12°, 15°, 30°, 60°, and 90° are shown (X-ray light curves are labeled), with the brighter peak fluxes reached by curves progressively closer to the jet axis. Light curves are plotted at 8.6 GHz radio (solid curves), V-band optical (dotted), and 3 keV X-ray (Dashed). Note how very dim off-axis transients are at X-ray and optical frequencies compared to on-axis events.

Beaming break when $\theta < 1/\Gamma \Rightarrow \Gamma_o \theta \approx (t_{br}/t_d)^{3/8}$

$$\Rightarrow t_{br} \approx 12\left(\frac{E_{52}}{n_{CBM}}\right)^{1/3}\theta^{8/3} days \Rightarrow \theta \propto t_{br}^{3/8}\left(\frac{n_{CBM}}{E_{52}}\right)^{1/8}$$

Evidence for constant energy reservoir

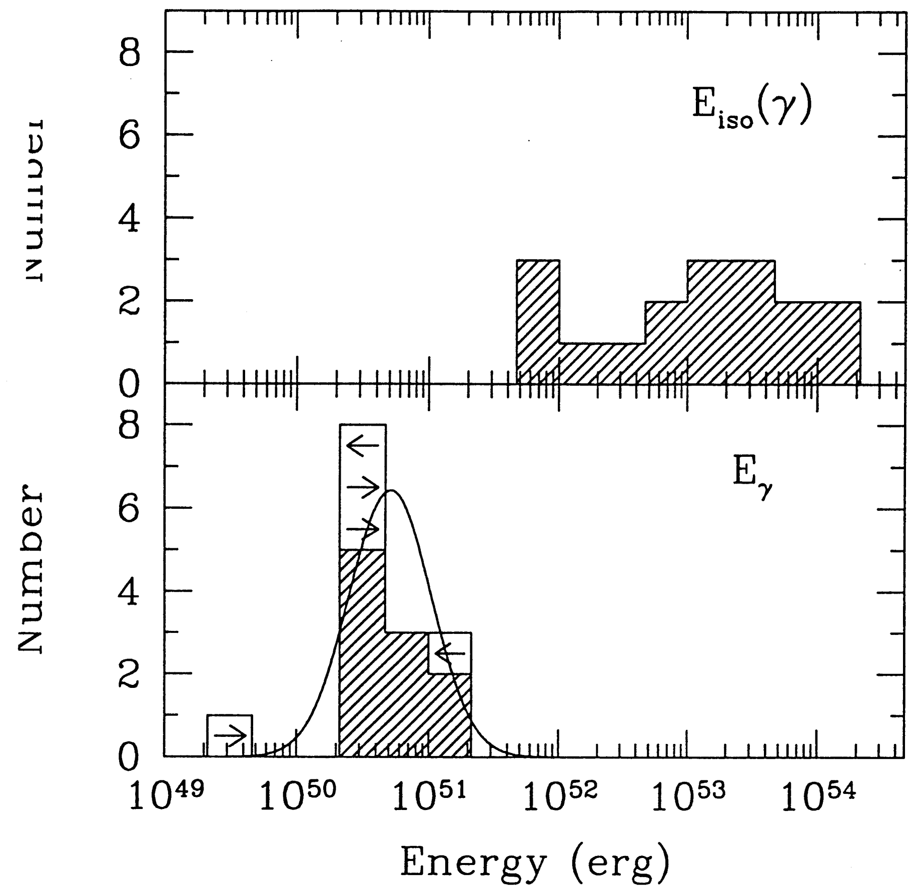

Frail et al. (2001)

$$E_{tot} \cong \frac{1}{4}\eta_\gamma \theta^2 E_\gamma(iso) \qquad \langle E_{GRB}\rangle \cong 3(\frac{\eta_\gamma}{3}) \times 5 \times 10^{50} ergs$$

GRB event rate > 500 x observed rate

Source Models

- Hypernova/Collapsar Model
  - Massive Star Collapse to Black Hole
  - Energy released at rotation axis
  - Two orders of magnitude more energy available; no prediction of constant energy reservoir
  - Requires active central engine
  - Does not admit (?) two-step collapse
  - Available number of sources

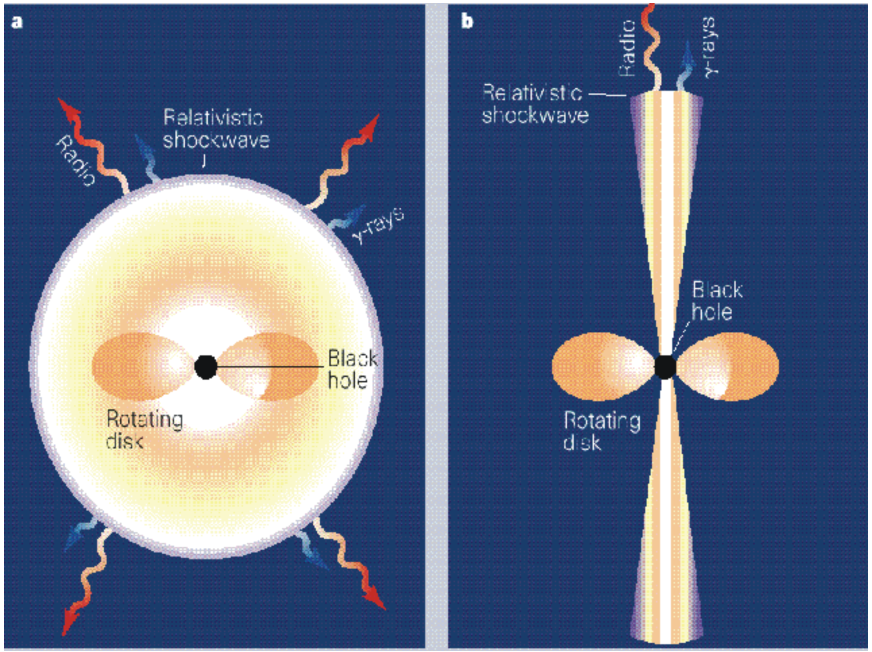

(Woosley et al.; Paczynski; Meszaros and Rees)

- Coalescing Compact Objects
  - Binary neutron stars known in Galaxy (Hulse-Taylor pulsar)
  - Coalescence by gravitational radiation
  - Expect ~1 coalescence event per Myr per MW Galaxy (too few given beaming fraction)
  - Prompt collapse
  - Expected to be found elliptical/non star-forming galaxies

Eichler et al. 1989; Janka, Ruffert et al.

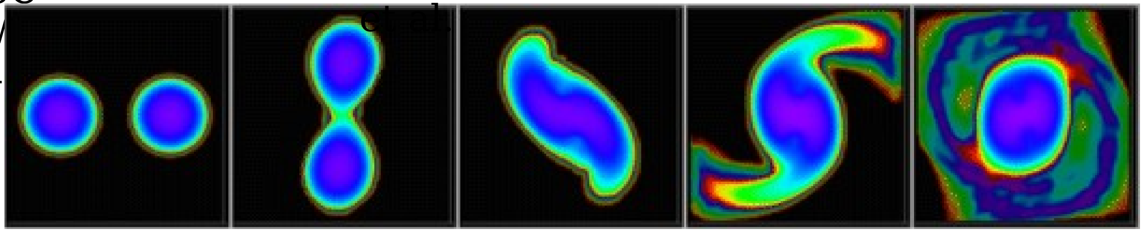

Connection of GRBs to Star Forming Regions and Supernovae

- Blue excesses in GRB host galaxies
- GRB optical counterparts coincident with center or spiral arms of galaxy hosts
- X-ray afterglows with no optical counterparts (due to extinction)

- Weak evidence for Fe $K\alpha$ line in X-ray afterglow spectra
- Spatial and temporal coincidence of GRB 980425 with SN 1998bw (Type Ic)
- Reddened supernova emission in late time optical afterglow spectra
- Energy release in constant energy reservoir is comparable to SN energy

Host galaxy of SN 1998bw

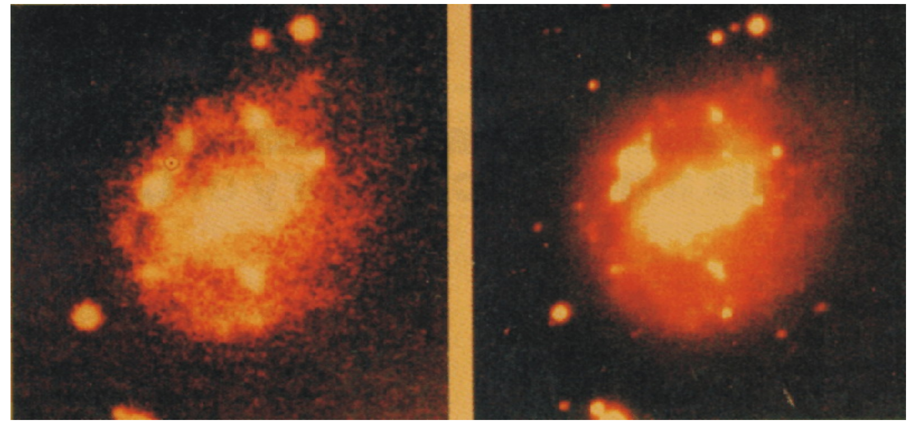

light curves of GRB 970228

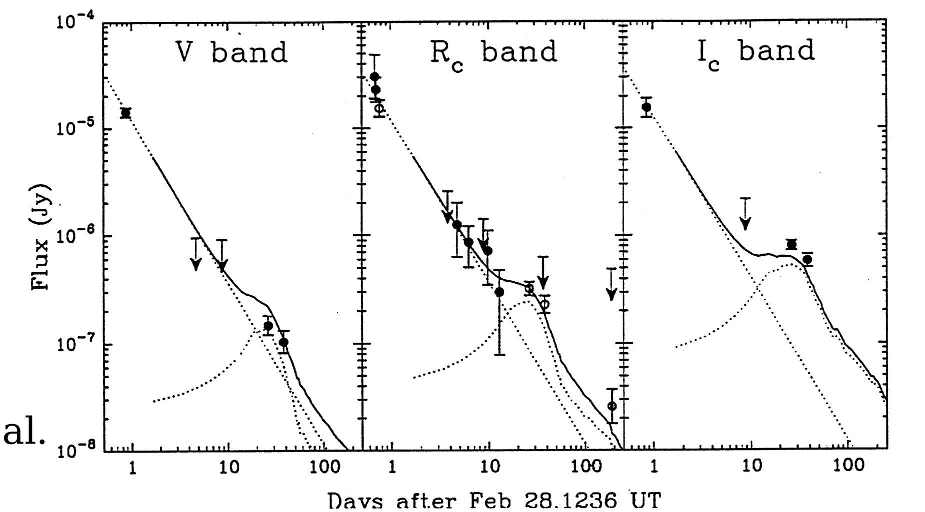

Galama et al.

X-ray features and the Supranova model

- Fe Kα fluorescence line emission in X-ray afterglow spectra, especially during rebrightening
- Fe absorption during the prompt phase (3σ)
- Optical rise associated with SN optical light curves
- Variable N_H

(Collapsar/hypernova model
Explains Fe Kα fluorescence
line emission due to active magnetar-
no black hole formation)

- Supranova model **(Vietri and Stella 1999)**
  - Two-step collapse to black hole
  - Super-Chandresekhar mass neutron star stabilized against prompt collapse by rotation
  - Supernova shell of enriched material
  - In dusty, star-forming regions
  - Explains rebrightening events
  - Standard energy reservoir
  - Prompt collapse following long quiescence

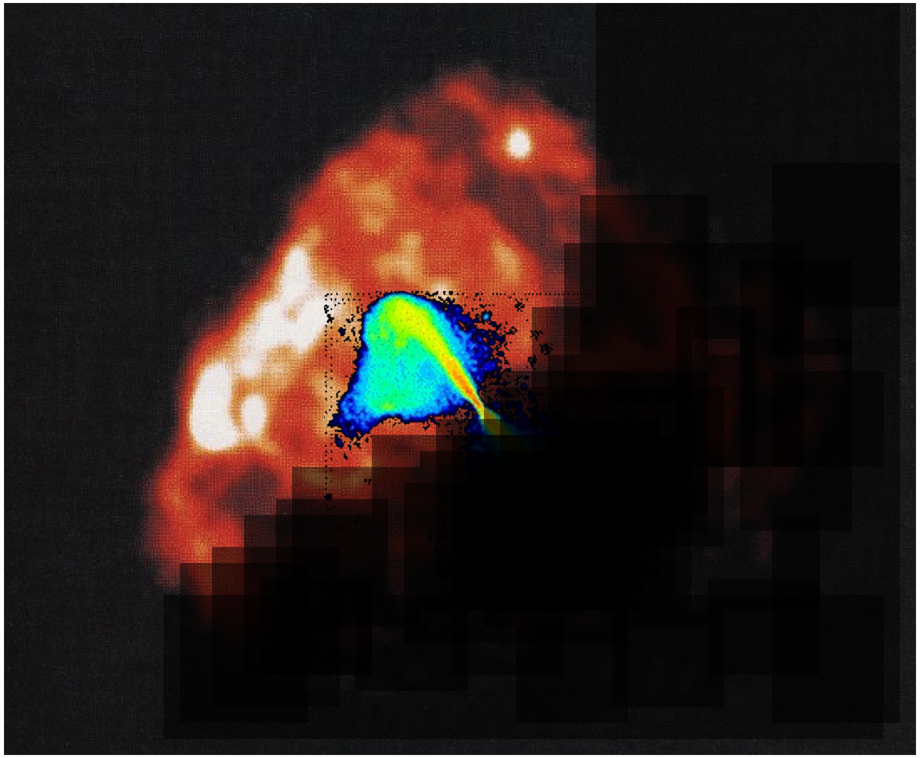

Rate and Power of GRBs into L* Galaxies

- **BATSE observations imply ~ 1 GRB/day over the full sky**
  - **Beppo-SAX GRBs represent long duration <t_{90}> > 2 s BATSE GRBs**
- **Redshift distribution peaks between 1 ~< z ~< 2**
- **Volume of the universe ~ 4π(4000 Mpc)^3 /3**
- **Density of L* galaxies ~ 1/(200-500 Mpc^3)**

Rate per L* galaxy

$$\approx \frac{500 Mpc^3 / L^*}{\frac{4\pi}{3}(4000 Mpc)^3} \frac{1}{day} \frac{365}{yr} \times 1000 f_3 \times SFR \times K_{FT}$$

$$\approx \left(\frac{SFR}{1/6}\right) \times \left(\frac{K_{FT}}{3}\right) \frac{f_3}{3.5 \times 10^{-4} yr} \approx f_3 / (3000 yrs)$$

Time-averaged power per L* galaxy

$$\approx \left(\frac{SFR}{1/6}\right) \times \left(\frac{K_{FT}}{3}\right) \times \frac{1.5 \times 10^{51} ergs}{2600 yrs \times 3 \times 10^7}$$

$$\approx 2 \times 10^{40} \left(\frac{SFR}{1/6}\right)\left(\frac{K_{FT}}{3}\right) ergs\, s^{-1}; \eta_\gamma = 1/3$$

K_{FT} correction factor for clean and dirty fireballs

Argument for the Supernova Origin of Cosmic Rays

- Local energy density of CR
  - $u_{CR} \cong$ 1 eV cm^{-3} $\approx 10^{-12}$ ergs cm^{-3}
- Cosmic ray power requirements
  - **$L_{CR} \cong u_{CR}V_{gal}/t_{esc} \approx 5\times10^{40}$ ergs s^{-1}**
- Galactic volume
  - $V_{gal} \approx \pi(15\ \mathrm{kpc})^2\times200$ pc ~ 1×10^{66} cm
- Cosmic ray escape time from galaxy
  - $t_{esc} \approx \Lambda/\rho c \approx 10$ gm-cm^{-2} / (m_p 1 cm^{-3} c) $\approx$ 6×10^6 yr
  - (information from ^{10}Be used to determine mean density $\Rightarrow$ smaller ρ and larger V_{ga}
- Galactic SN luminosity: 1 SN/ 30 yrs $\times$ ~10^{51} ergs in injection energy $\Rightarrow$
  - **$L_{SN} \cong 10^{42}$ ergs/s**

Caveat emptor

astro-

COSMIC RAY ENERGY SPECTRA

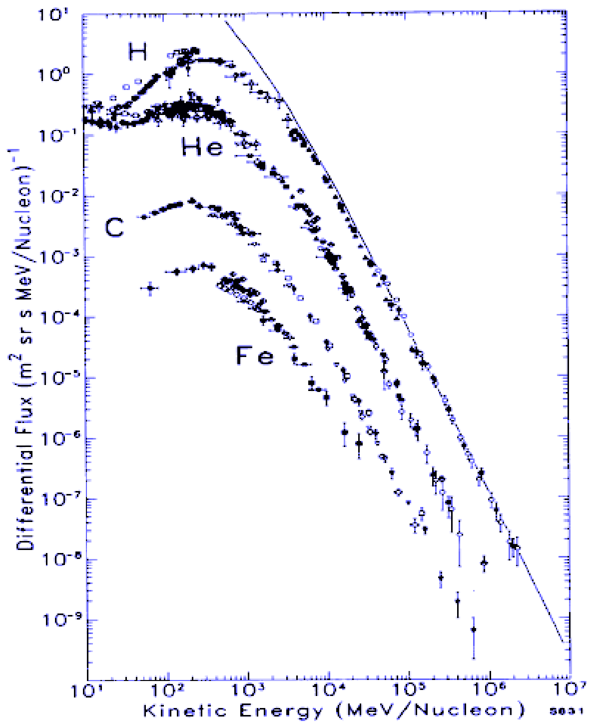

Figure 2. The differential energy spectra of the primary cosmic ray H, He, C, and Fe at Earth. [*Reproduced with permission from J. A. Simpson (1983). Ann. Rev. Nucl. Part. Sci. 33 by Annual Reviews, Inc.*].

COMPOSITION INDEPENDENT OF COSMIC RAY ENERGY/NUCLEON From ~ 1 to ~1000 GeV/Nucleon

Rates of various types of SNe

Table 1. Supernova and Fireball-Transient Rates in Supernova Units[a]

	Supernova and Fireball-Transient Types					
Galaxy Type	SN Ia	SN II	SNIb/c	FT	Total	Age Index
	N1	*N2*	*N3/N4*	*NF*		
E-S0	0.05±0.02	< 0.02	< 0.01	⋯	0.05±0.03	> 1.7
S0a-Sb	0.10±0.04	0.24±0.11	0.06±0.03	⋯	0.40±0.24	0.33±0.16
Milky-Way type: Sbc-Sd	0.21±0.08	0.86±0.35	0.14±0.07	~0.05	1.21±0.64	0.21±0.11
Sm, Irr	0.59±0.24	0.97±0.60	0.33±0.24		1.89±1.12	0.45±0.3
	Progenitor Mass Ranges					
	$\lesssim 8\ M_\odot$	$\sim$ 6-30 $M_\odot$	$\sim$ 20-80 $M_\odot$	$\gtrsim 60\ M_\odot$		

[a]multiply by factor of ~2 to get the SN rate per century in the Milky W

Detection of hadronic emission from SNRs

Intensity of SNR gamma-ray sources with EGRET:

$$\frac{10^{51} ergs/SN \times efficiency\,\eta_p \times c\sigma_{pp} n_{ISM} \times 140\,MeV}{(2\times 10^{-3} f_{norm}\, ergs/CR)\,4\pi R^2}$$

$$\cong 10^{-11} \left(\frac{f_{norm}}{10}\right)^{-1} \left(\frac{\eta_p}{0.1}\right) n_{ISM} R_{kpc}^{-2}\, ergs\, cm^{-2} s^{-1} \quad at\, 100\, MeV$$

Intensity of SNR gamma-ray sources with Cherenkov telescopes:

$$\cong (10^{-13} - 10^{-11}) \times \left(\frac{f_{norm}}{10}\right)^{-1} \times \left(\frac{\eta_p}{0.1}\right) n_{ISM} R_{kpc}^{-2}\, ergs\, cm^{-2} s^{-1} \quad at\, 1\, TeV$$

Sensitivity of High Energy Telescopes

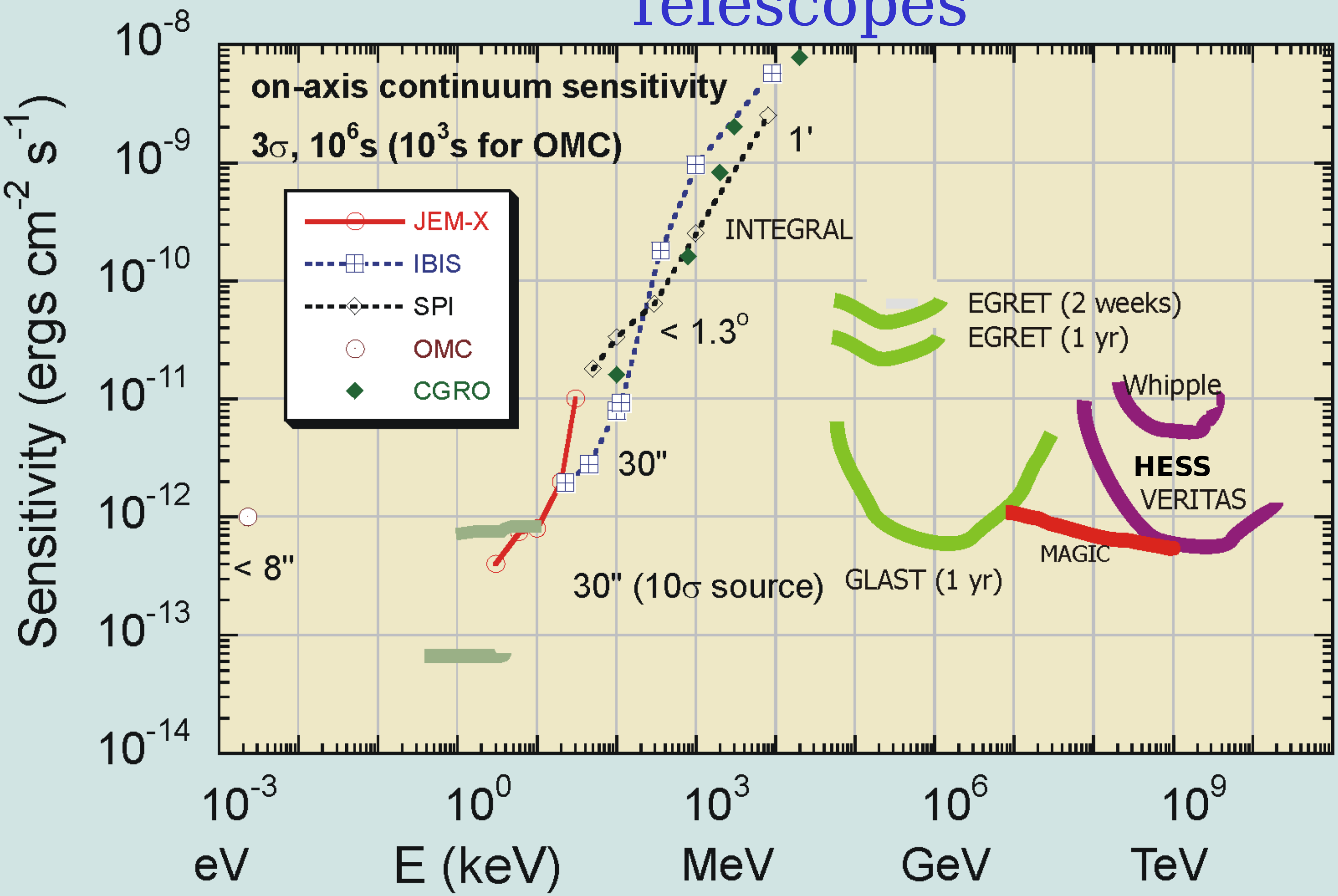

HEGRA detection of Cas A: shell-type SNRs do not (?) power galactic CRs

(Aharonian et al. 2001)

Particle Acceleration at Astrophysical Shocks

- **Nonrelativistic and relativistic shock-Fermi mechanism is incapable of accelerating particles to the ankle (~10^{19} eV) of the cosmic ray spectrum**
- **Redo calculation of Lagage and Cesarsky with Combined 1st and 2nd order Fermi acceleration and for nonrelativistic and relativistic shocks**
    - **Please see Vol. 6, OG, p. 2039**

$$E_{\max,I} \approx 10^{16} Z B_{\mu G} \beta_0^{2/3} \left(\frac{m_o \Gamma_0}{n_{ext}}\right)^{1/3} eV$$

$$E_{\max,II} \approx 8\times 10^{20} Z K_v e_B^{1/2} n_{ext}^{1/6} f_\Delta (m_o \Gamma_0)^{1/3} eV$$

$$K_v = [2^{3/2} e_B \xi \beta_o / 9 f_\Delta]^{1/(2-v)} \quad \propto \quad \beta_0^2 (v=3/2), \beta_0^3 (v=5/3)$$

It is proposed that Fermi processes in relativistic flows formed by stellar collapse (either one- or two-step) events power the cosmic rays from the knee to ultra-high energies

Maximum Particle Acceleration at Nonrelativistic and Relativistic Shocks

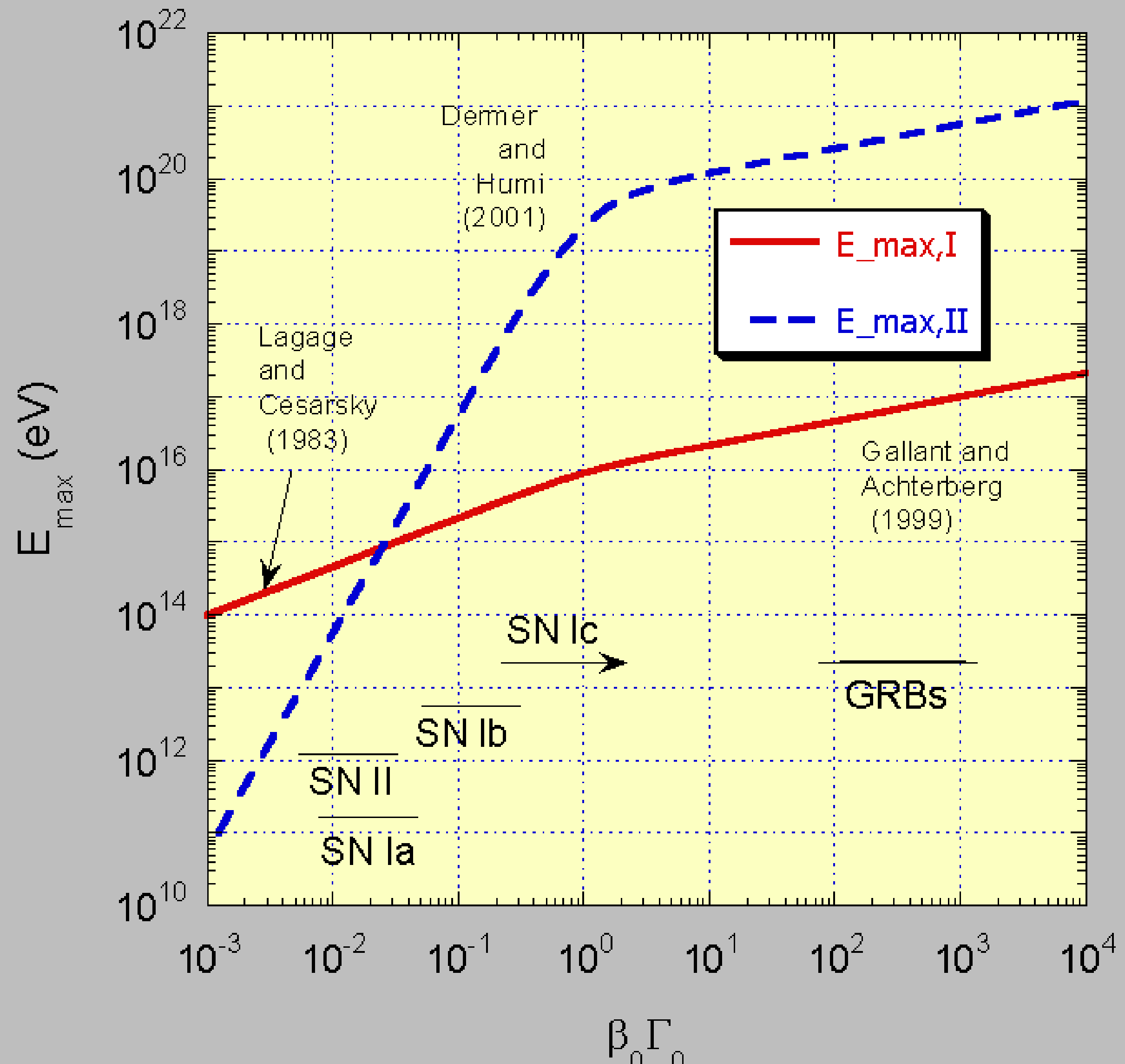

UHECRs from GRBs

Vietri (1995), Waxman (1995), Milgrom and Usov (1995)

- Typical fluence and rate of BATSE GRBs:
  - $F_\gamma \approx 3\text{x}10^{-6}$ ergs cm^{-2} ; $N_{GRB} \approx 1$/day
- If weakest GRBs at $z \sim 1$, then $d \cong 10^{28}$ cm $\quad V_{trap} \approx 4\pi d^3/3$
- $E_\gamma \approx 4\pi d^2 F_\gamma (1+z) \approx 8\text{x}10^{51}$ ergs; $E_{GRB} \approx 10^{53}$ ergs $\Rightarrow L_{GRB} \approx 10^{48}$ ergs/s
  - UHECRs lose energy due to photomeson processes with CMB
  - $p + \gamma \rightarrow p + \pi^0$, $n + \pi^+$
  - GZK Radius $x_{1/2}(10^{20}$ eV$) \cong$ 140 Mpc
    - (Stanev et al. 2000)
  - $\Rightarrow t_{esc} \approx 1.5\text{x}10^{16}$ s
- Energy density within GZK Radius:
  - $u_{UHECR} \cong \eta\, \varepsilon_{GRB} (x_{1/2}/c) \cong \dfrac{\eta L_{GRB}\; t_{esc}}{(4\pi/3)(10^{28}\text{cm})^3}$

$\cong \eta\; 5\times10^{-21}$ ergs/cm^3

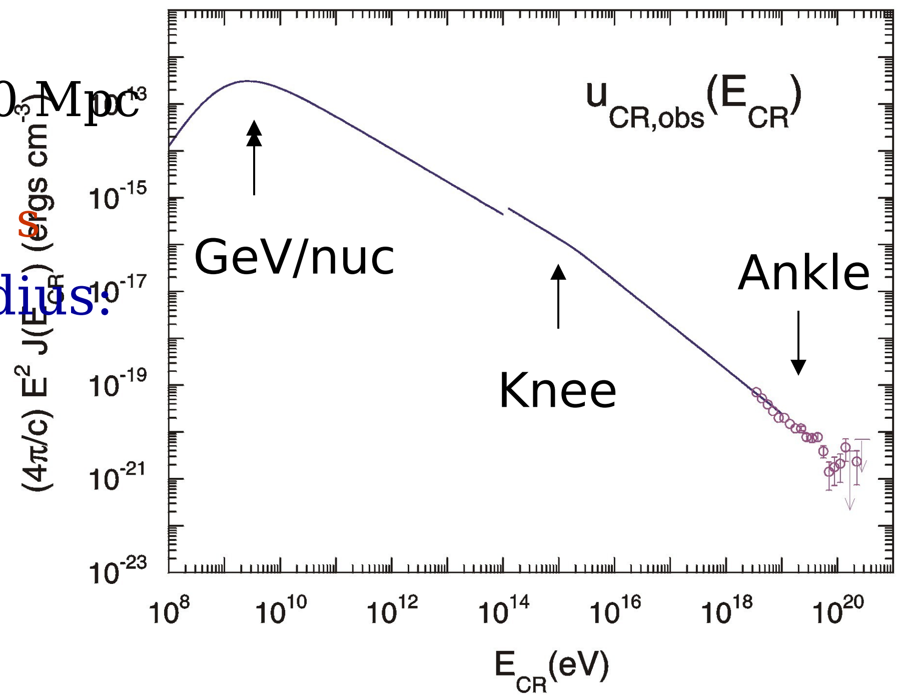

Böttcher & Dermer (ApJ, 2000, 529, 635)

Cosmological Statistics of GRBs in the External Shock Model

- Assume that distribution of GRB progenitors follows star formation history of universe
  Trigger on 1024 ms timescale using BATSE trigger efficiencies (Fishman et al. 1994)
- Broad distributions of baryon-loading Γ_0 and directional energy releases are required. Assume power laws for these quantities.
  - $10^{-6} < E_{54} < 1$; $N(E_{54}) \propto E_{54}^{-1.52}$; $\Gamma_0 < 260$; $N(\Gamma_0) \propto \Gamma_0^{-0.25}$

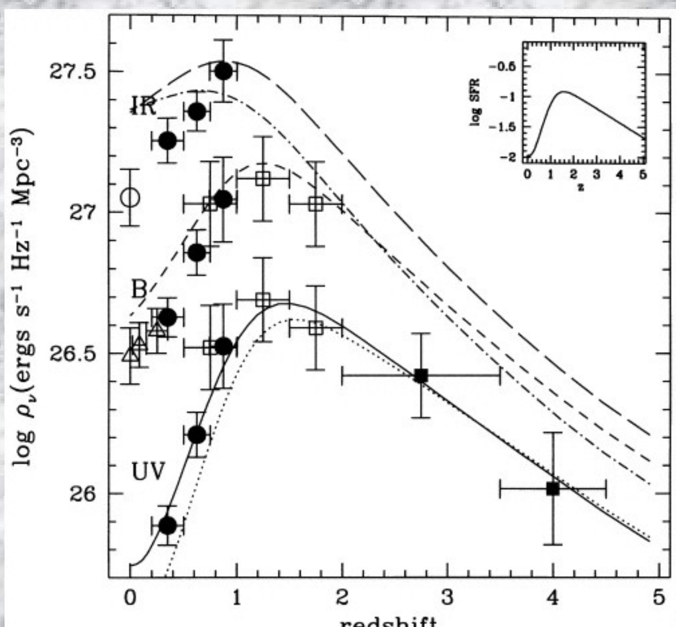

(Madau et al. 1998)

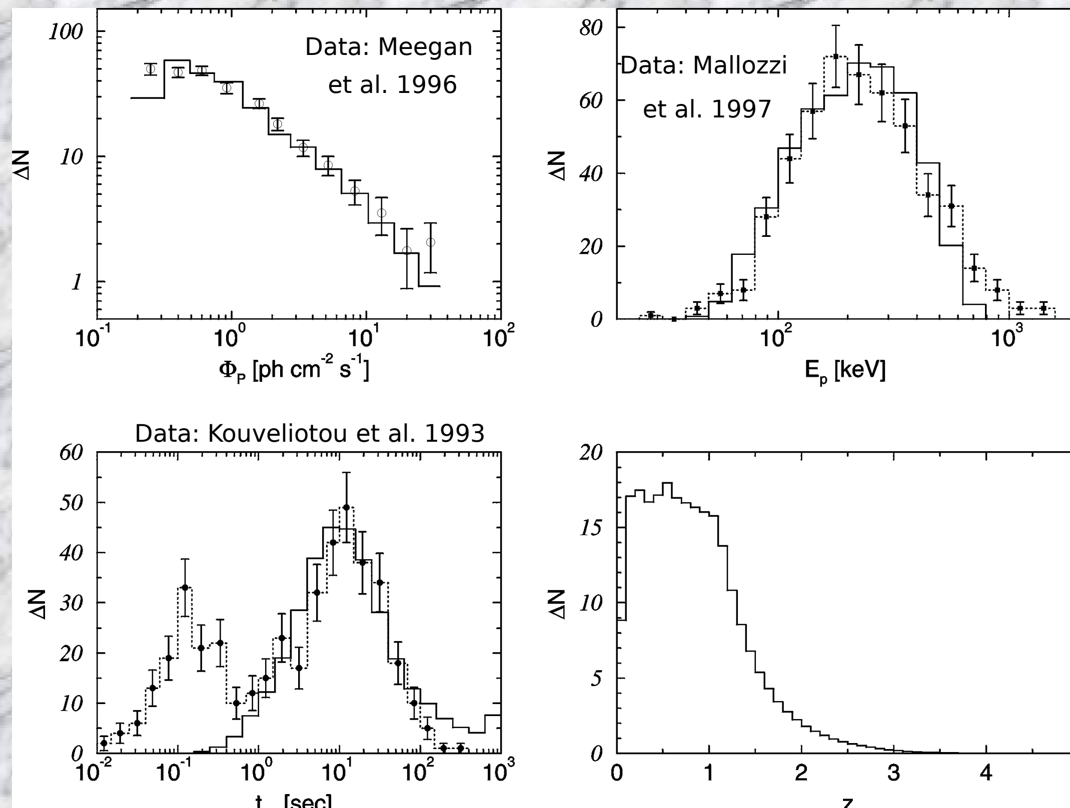

astro-ph/0005440
application to UHECRs

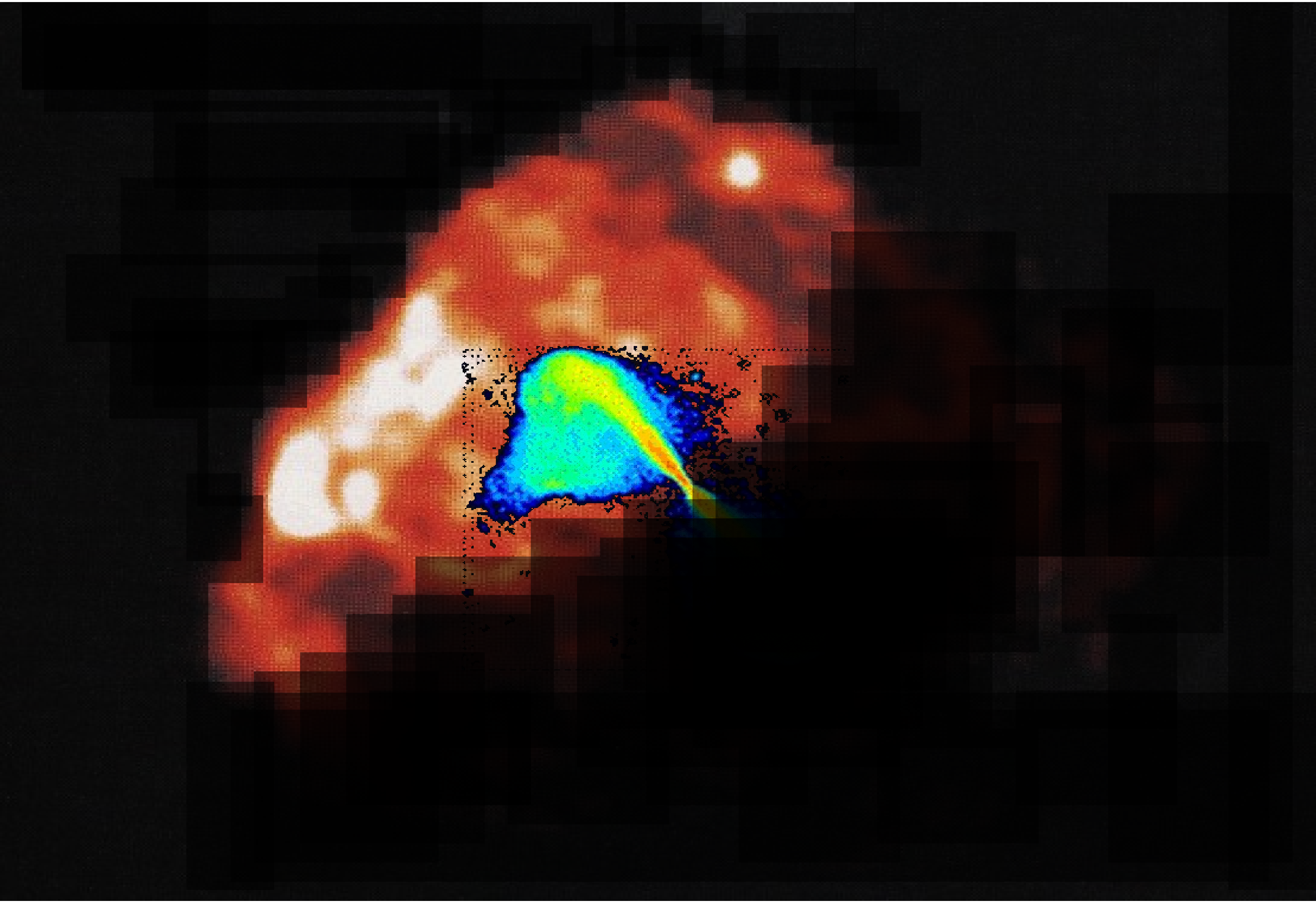

Short Timescale Variability due to inhomogeneities in surrounding medium

- Clouds with thick columns (>~ 4×10^{18} cm^{-2})
  - Total cloud mass still small (<<10^{-4} M_o)
- Cloud radii << R/Γ

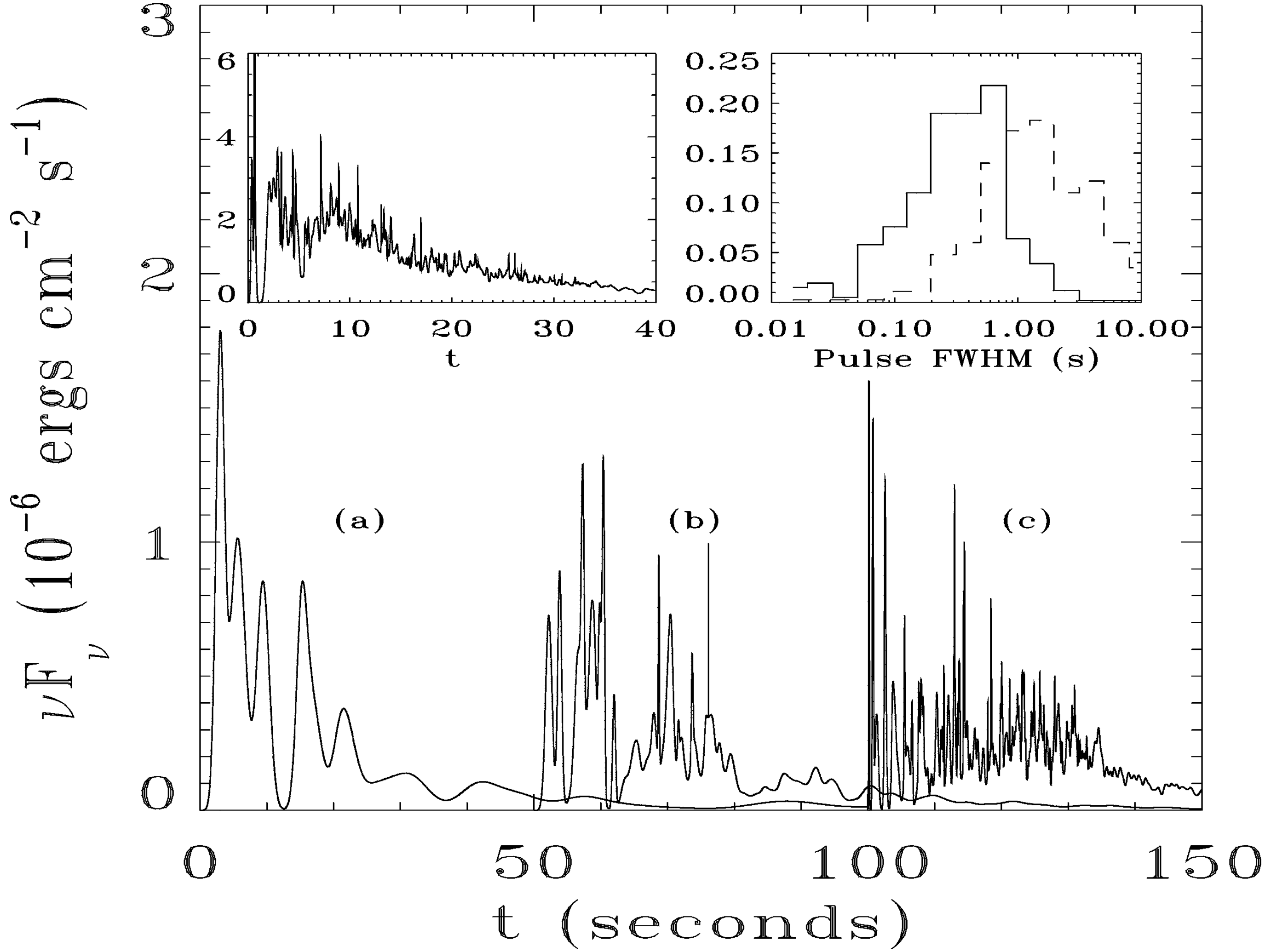

Gamma Ray and Neutrino Production

- Low neutrino luminosity in uniform surrounding environment
- Collision of relativistic blast wave with dense shell reduces expansion losses of swept-up particles
- High-target density and backscattered photons produce strong photomeson (Atoyan and Dermer 2001) and secondary production signatures
- Nonthermal neutral beam outflow in collapsing stars would be traced by γ-ray pair halo (Coppi, Aharonian, and Völk 1994)
- Buried γ-ray and ν sources depending on delay time, mass and clumpiness of SNR shell
- UHECRs from escaping neutrons
- γ-cascade radiation pileups from 10-1000 TeV photons produced in photomeson processes that cascade to unity $\tau_{\gamma\gamma}$ =1 optical depth of the universe
- Diffuse γ-cascade radiation pileup at 30-200 GeV

Advanced Blast Wave Theory

- **Neutron decoupling in fireball (Derishev et al.)**
- **Backscattered radiation; formation of pair fronts (Beloborodov)**
- **Joint forward and reverse shock analysis**
- **Relativistic shock hydrodynamics and particle acceleration in clumpy media**
- **UHECR production, neutron escape, and the formation of neutron-decay halos (astro-ph/0005440)**

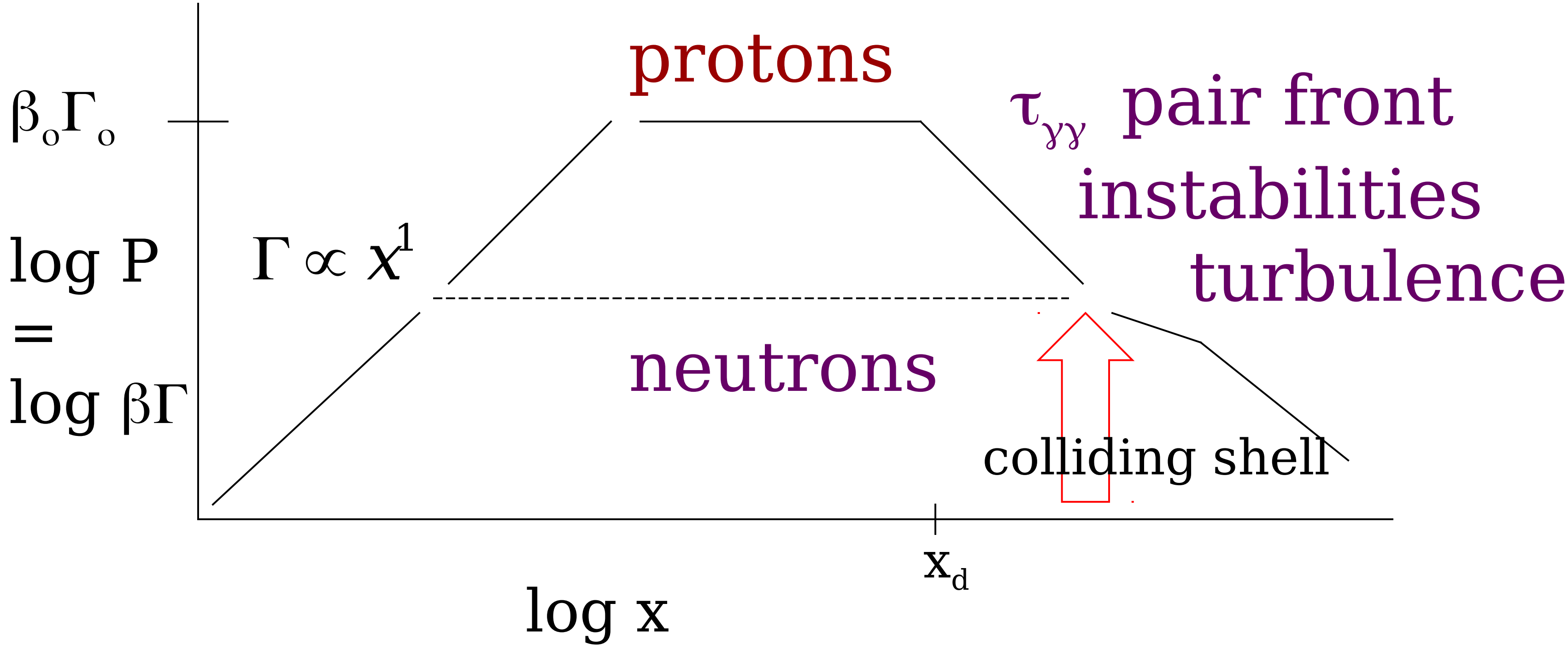

No Observational Evidence for Hadronic CR Component

- Unidentified EGRET sources are not firmly associated with SNRs and do not display π^0 features; now appear more likely to be pulsars
- TeV γ rays not detected at expected levels
- Diffuse galactic γ-ray background spectrum harder than expected from locally observed CRs
- Single source model for origin, composition, and spectrum of CRs at and above the knee of the CR spectrum appears to be ruled out by Kascade results

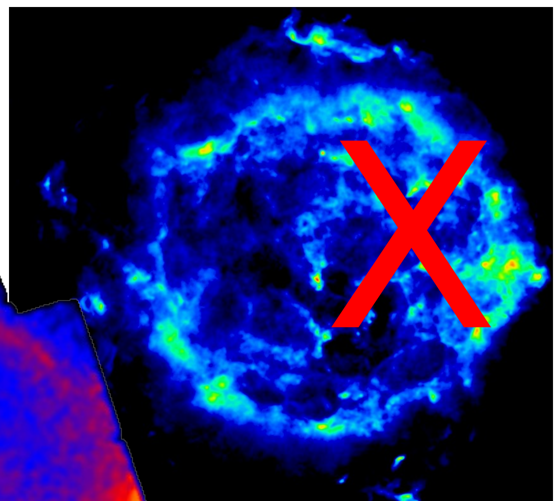

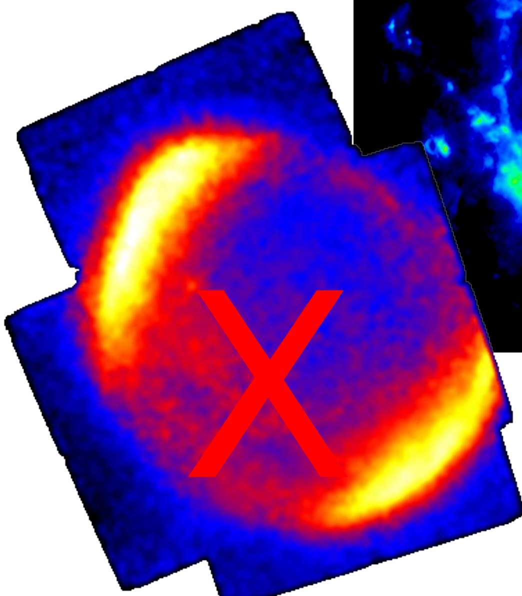

To be considered:

If cosmic rays do not originate
from SN 1a and SN II, then
from SN 1b/c and GRBs

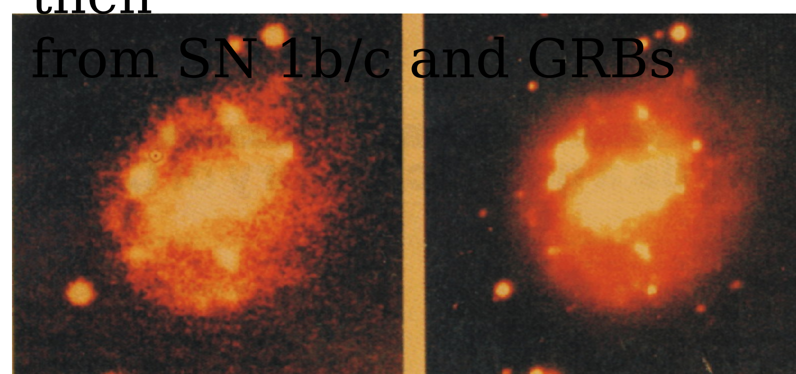

1. Host galaxy studies reveal galaxies that are sites of ongoing (and obscured) star formation in the early universe
2. Dust content and relationship between ULIGs (> 10^{13} $L_\odot$ in IR), Scuba sources, and GRB host galaxies (Trentham)
3. Metallicity effects—Pop III stars at high redshifts
4. Black hole population in the universe: growth and census
5. Geometrical effects on SN light curves due to directional dust obscuration (Trentham)

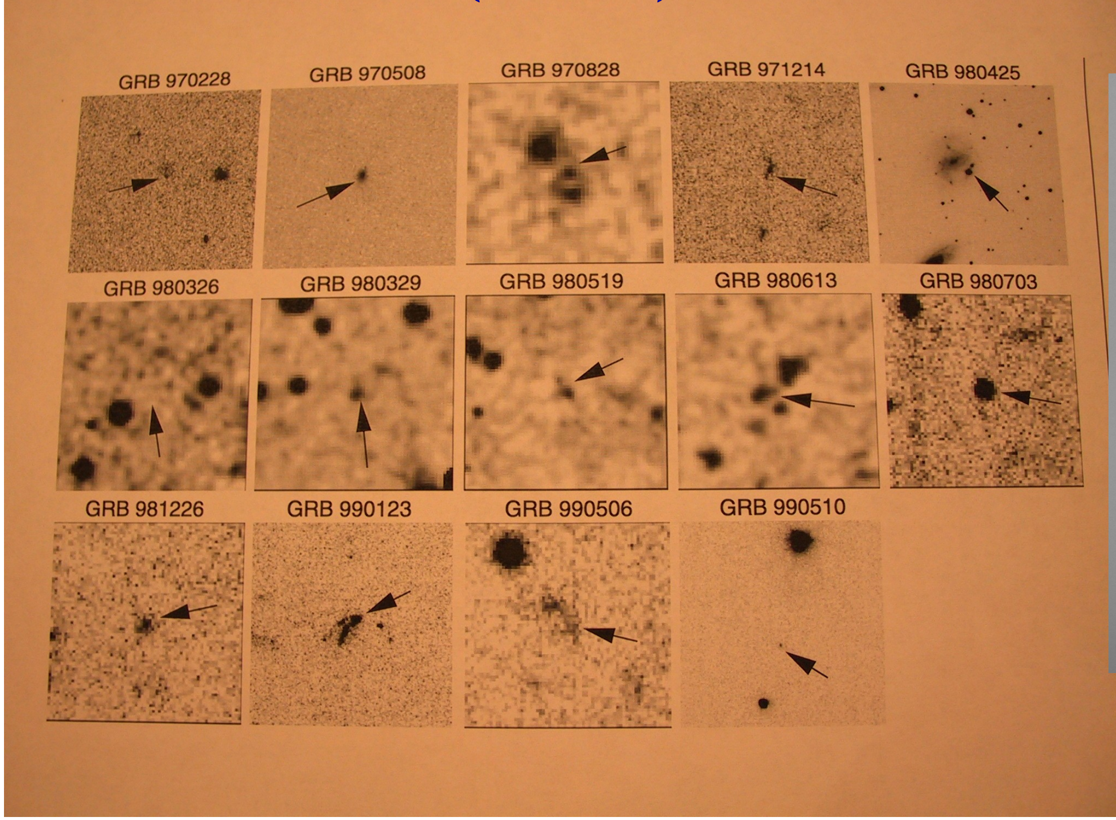

GRB cosmology

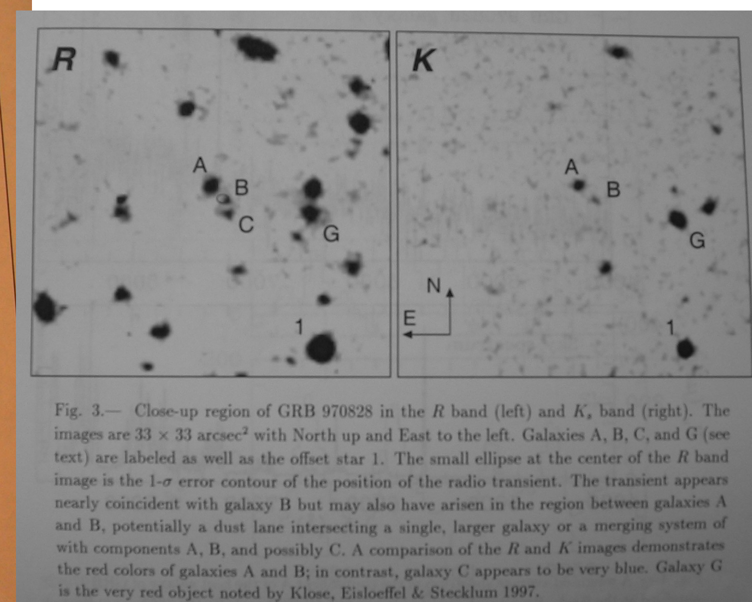

Points to take with you

1. Supranova model preferred by X-ray data over collapsar model
2. Two-step collapse process favors impulsive GRB power sources
3. Highly clumped environment leads to complicated behaviors
4. Pts. 2 and 3 support external shock model for GRBs
5. Relativistic flows accelerate particles to > 10^{20} eV (through 2nd order processes)
6. Rate of supernova events accompanying GRB events occurs at a rate of 1 per 2-4 millenia throughout the Milky Way
7. (Look for beamed signatures in galactic SNe; hadronic signatures in 1 out of ~20 SNRs)
8. Time and space-averaged power of relativistic flows into Milky Way from GRB events that accompany supernova is ~10^{40} ergs s^{-1}
9. GRBs potentially power the UHECRs
10. Relativistic flows in the galaxy associated with GRB events can accelerate CRs in the regime between the knee and ankle (assumed to be confined to the Milky Way's halo)
11. GRBs could accelerate a substantial fraction of the locally observed cosmic rays
12. Thus

the hypothesis that CRs originate from particle acceleration in SNRs powered by SNe in the galaxy, is suggested to be replaced with the hypothesis that

CRs originate from the stars that produce the subclass (SN Ic?) of SNe whose core collapses a second time to a black hole which powers relativistic flows and GRBs

The

E

n

d

Points to take with you

1. **Supranova model preferred by X-ray data over collapsar model**
2. **Two-step collapse process favors impulsive GRB power sources**
3. **Highly clumped environment leads to complicated behaviors**
4. **Pts. 2 and 3 support external shock model for GRBs**
5. **Relativistic flows accelerate particles to > 10^{20} eV (through 2nd order processes)**
6. **Rate of supernova events accompanying GRB events occurs at a rate of 1 per 1-2 millenia throughout the Milky Way**
7. **(Look for beamed signatures in galactic Sne; 1 out of ~10-20 young SNRs are powerful hadronic sources)**
8. **Time and space-averaged power of relativistic flows into Milky Way from GRB events that accompany supernova is ~10^{40} ergs s^{-1}**
9. **GRBs potentially power the UHECRs**
10. **Relativistic flows in the galaxy associated with GRB events can accelerate CRs in the regime between the knee and ankle (assumed to be confined to the Milky Way's halo)**
11. **GRBs could accelerate a substantial fraction of the locally observed cosmic rays**
12. **Thus the hypothesis that CRs originate from particle acceleration in SNRs powered by SNe in the galaxy, is suggested to be replaced with the hypothesis that**

    CRs originate from the stars that produce the subclass (SN Ic?) of SNe whose core collapses a second time to a black hole which powers relativistic flows and GRBs


Blast Wave Physics in a Realistic Environment

Prompt optical emission from the reverse shock

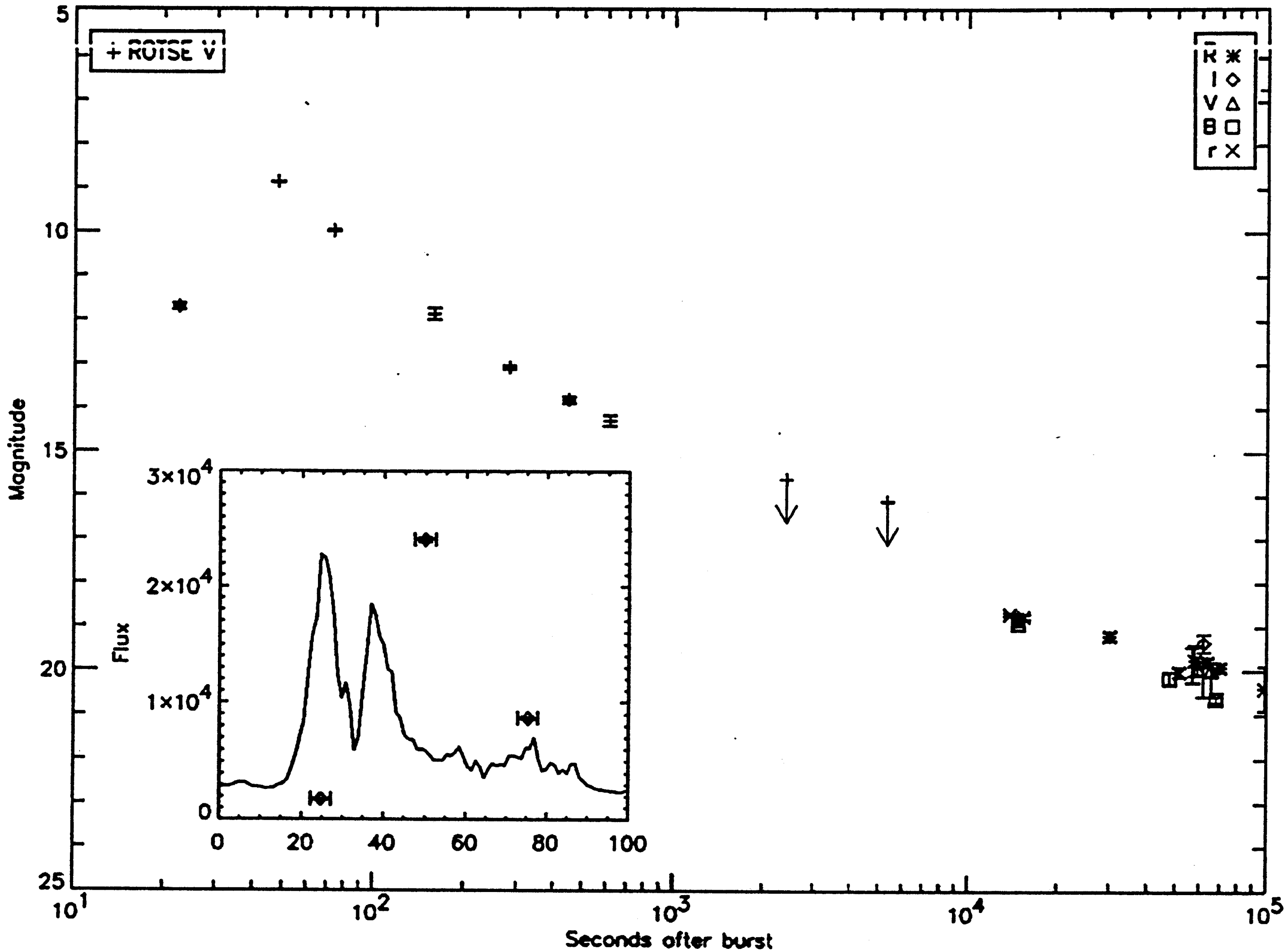

App. GRB 970828 optical image

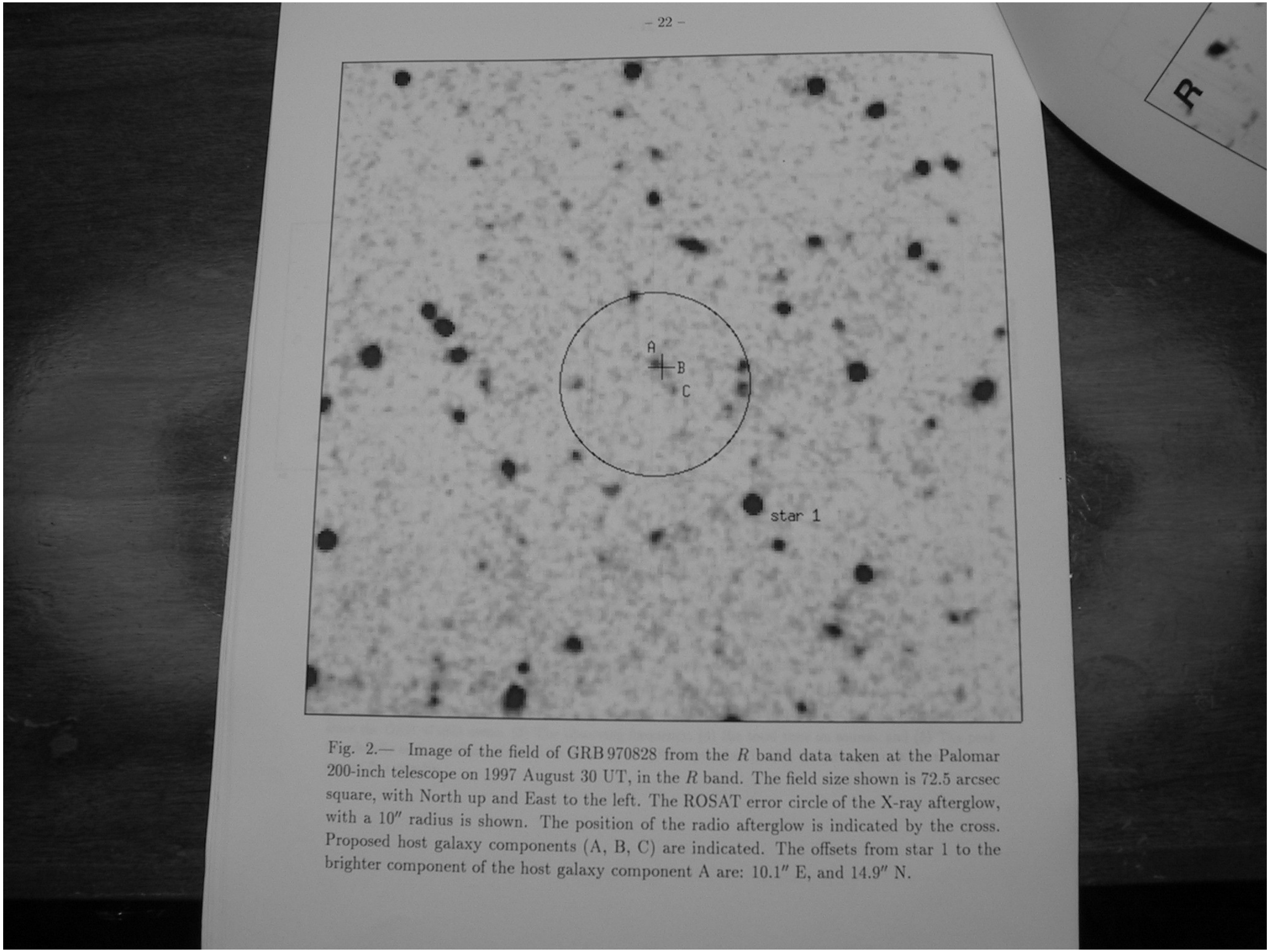

– 22 –

A
B
C
star 1

Fig. 2.— Image of the field of GRB 970828 from the R band data taken at the Palomar 200-inch telescope on 1997 August 30 UT, in the R band. The field size shown is 72.5 arcsec square, with North up and East to the left. The ROSAT error circle of the X-ray afterglow, with a $10''$ radius is shown. The position of the radio afterglow is indicated by the cross. Proposed host galaxy components (A, B, C) are indicated. The offsets from star 1 to the brighter component of the host galaxy component A are: $10.1''$ E, and $14.9''$ N.

Tables of redshifts, jet break times, and energetics (Frail et al. astro-ph/0102282)

The

GRB	F_γ	z	d_L	$E_{\rm iso}(\gamma)$	t_j	θ_j	E_γ	Refs.	Note
970228	11.0	0.695	1.4	22.4					N
970508	3.17	0.835	1.8	5.46	25	0.293	0.234	36	R
970828	96.0	0.958	2.1	220	2.2	0.072	0.575	62	X
971214	9.44	3.418	9.9	211	> 2.5	> 0.056	> 0.333	63	O
980613	1.71	1.096	2.5	5.67	> 3.1	> 0.127	> 0.045	64	O
980703	22.6	0.966	2.1	60.1	7.5	0.135	0.544	65	B
990123	268	1.600	3.9	1440	2.04	0.050	1.80	14	O
990506	194	1.30	3.0	854					N
990510	22.6	1.619	4.0	176	1.20	0.053	0.248	18	B
990705	93	0.84	1.8	270	~ 1	0.054	0.389	66	O
990712	6.5	0.433	0.8	5.27	> 47.7	> 0.411	> 0.445	67	O
991208	100	0.706	1.4	147	< 2.1	< 0.079	< 0.455	68	D
991216	194	1.02	2.3	535	1.2	0.051	0.695	34	O
000131	41.8	4.500	13.7	1160	< 3.5	< 0.047	< 1.30	69	D
000301C	4.1	2.034	5.3	46.4	5.5	0.105	0.256	5	B
000418	20.0	1.119	2.5	82.0	25	0.198	1.60	35	B
000926	6.2	2.037	5.3	297	1.45	0.051	0.379	70	O

17

Table 1. Jet Break Times and Energetics. The gamma-ray fluences (F_γ), given in uni
erg cm^{-3}, are from a diverse collection of instruments. The best determinations of energy fluenc
the *Burst and Transient Experiment* (BATSE) on the *Compton Gamma Ray Observatory* (CG

SN excess emission in GRB afterglow light curves

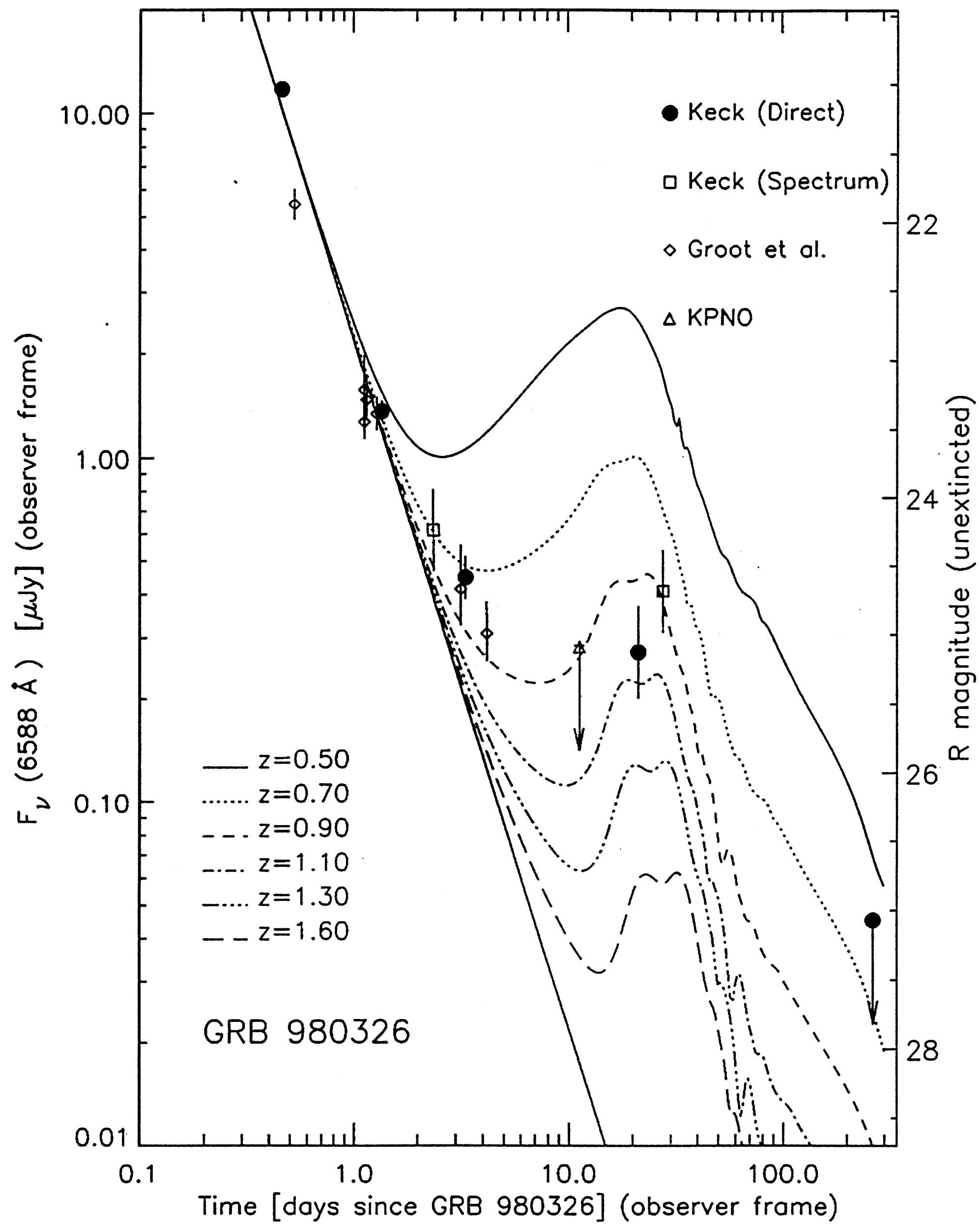

Theory of Gamma Ray Bursts

C. D. Darmer

the United States

ψ